POLITECNICO DI TORINO

Master's Thesis in Biomedical Engineering

Electrospun cellulose acetate fibers: a new approach for *in vitro* models of the blood-brain barrier

Supervisor
Danilo Demarchi
Co-supervisor
Gianni Ciofani
Elisa Mele

Candidate
Umberto Buratti
s238940

Polytechnic University of Torino

Department of Mechanical and Aerospace Engineering Academic Year 2018/2019

ISTITUTO ITALIANO
DI TECNOLOGIA
SMART BIO-INTERFACES

Index

1 Introduction

1.1 Statement of purpose and overview

This thesis aimed to investigate a new approach for the realization of *in vitro* models of the blood-brain barrier (BBB). The attention was focused on the development of a protocol whose costs and time requirements were suitable for high-throughput analysis and studies, exploiting electrospinning technology. Firstly, porous substrates made of electrospun fibers of cellulose acetate were realized and their morphological characteristics assessed. Subsequently, a static cellular mono-culture of endothelial cells was conducted in order to obtain the *in vitro* model. The reliability of the model was then investigated both through the analysis of TEER and permeability values, and through confocal imaging.

1.2 The blood-brain barrier (BBB)

Within the central nervous system (CNS), substance exchanges between blood and neural tissue are regulated by three barrier layers set at key interfaces [1]:

- The blood-brain barrier (BBB), made of the endothelial cells forming the walls of the capillaries
- The blood-cerebrospinal fluid barrier (BCSFB), made of the epithelial cells of the choroid plexus facing the cerebrospinal fluid
- The avascular arachnoid epithelium

These combined layers function as a physical, transport and metabolic barrier, in summary both providing a stable fluid environment needed by neural functions and protecting the CNS from chemical damage. The BBB represents a highly selective and specific barrier and is by far the largest of the three layers, due to the combined area of the microvessels composing it [2].

The first steps of the discovery of the BBB date back to the beginning of 20th century, with the work of the bacteriologist Paul Ehrlich. Studying the procedure of staining, he discovered that the chemical dyes injected in animal corpses to make fine biological structures visible reached all organs except for the brain. However, Ehrlich attributed this result to a limited affinity of the brain for the dye used. In 1913 Edwin Goldman, one of Ehrlich's students, observed that the same dyes coloured neural tissue once directly injected into subarachnoid space. This falsified the hypothesis that the differences in staining were due to a lower affinity of tissues for the dyes, and eventually led to the conclusion that the dye was unable to cross the walls of brain capillaries. These experiments were the first to bring about the concept of a barrier between the brain and blood [3].

1.2.1 Structure and function of the BBB

The term "blood-brain barrier" defines the characteristics of the vasculature of the central nervous system, composed of continuous nonfenestrated microvessels that, due to their characteristics, are able to precisely control the movements of molecules, ions and cells [4]. The barrier functions of the BBB are

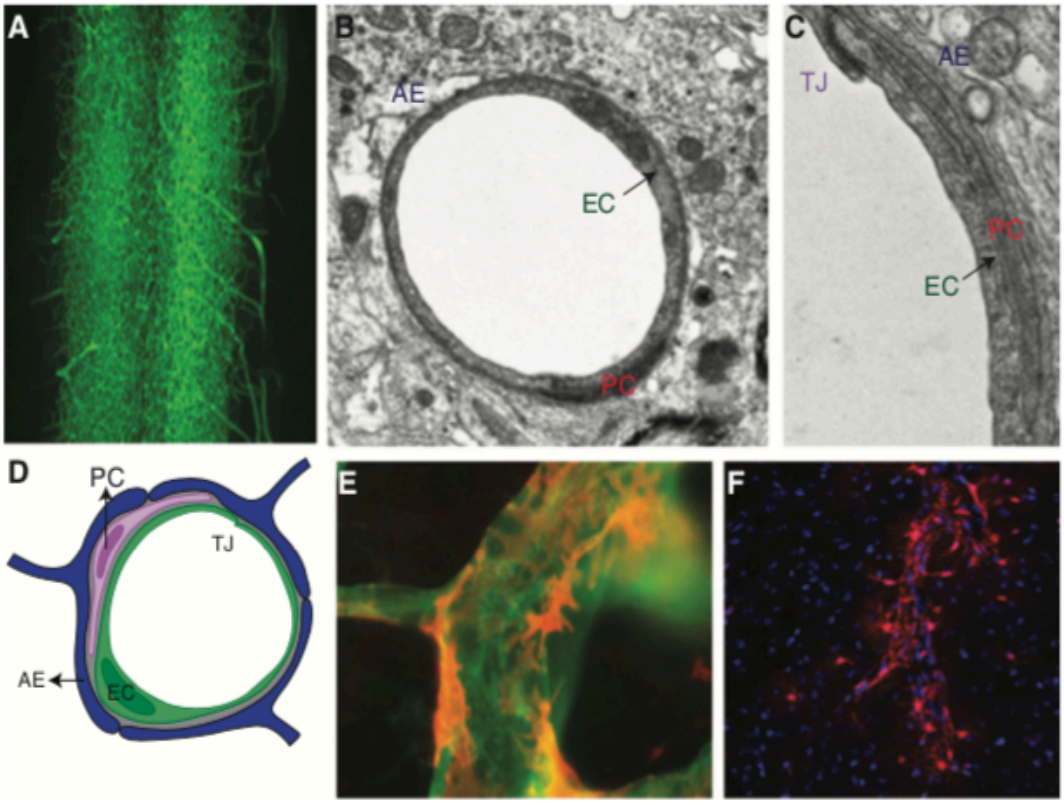

Figure 1. *Components of the BBB. (A) Vascular cast of a spinal cord showing density of the CNS vascular network. (B) Electron micrograph (EM) of a cross section of a CNS vessel depicting a connection between endothelial cells (ECs), pericytes (PCs), and astrocytes. (C) Magnified EM of ECs depicting a connection between ECs (with tight junctions [TJ]), PCs, basement membranes (BMs), and astrocyte endfeet (AE). (D) Schematic representation of the cell types within the neurovascular unit. (E) Immunofluorescence micrograph depicting a connection between PCs (red) and ECs (green). (F) Micrograph depicting a connection between astrocytes (red) and blood vessels (unstained) [5].*

largely due to the endothelial cells forming the walls of the CNS blood vessels. However, interactions with other cells composing the neurovascular unit induce and maintain those functions: mural cells, immune cells, glial cells and neural cells (Figure 1) [5].

The term mural cells refers to vascular smooth muscle cells, surrounding larger vessels, and pericytes, that sit on the abluminal surface of the microvascular endothelial tube [6]. Pericytes play a crucial role in both regulating the generation of the barrier during the period of development and maintaining its function in aging [7]. The vascular tube is surrounded by two basement membranes (BMs): the inner vascular BM, secreted by the endothelial cells and

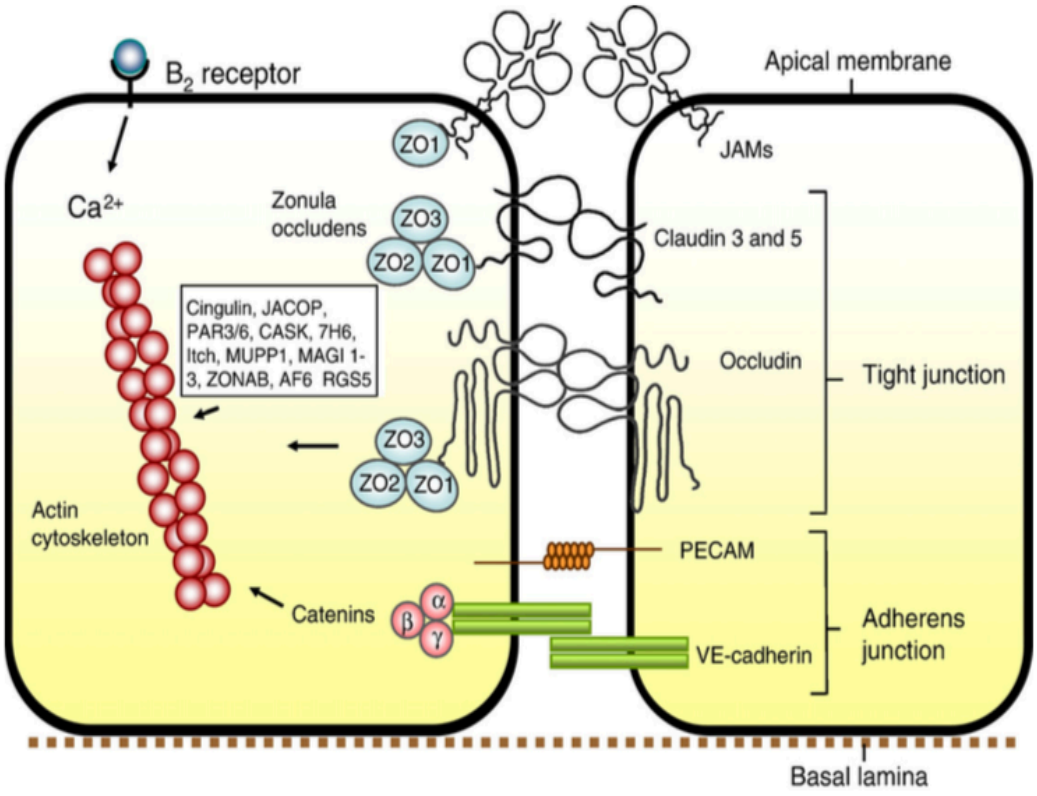

Figure 2. *Structure of BBB tight junctions. The tight junctional complex comprises occluding and claudins. Cadherins of the adherent junctions provide structural integrity and attachment between the cells, and are necessary for formation of tight junctions. Selective barrier diffusion and high electrical resistance of the BBB appear to be largely due to the properties of claudins. The claudins and occludin are linked to the scaffolding proteins ZO-1, ZO-2 and ZO-3, linked in turn via cingulin dimers to the actin/myosin cytoskeletal system within the cell [10].*

pericytes, and the outer parenchymal BM. Both together form an additional barrier layer that molecules and cells have to cross before entering the neural tissue [8]. Astrocytes are a glial cell type that form a connection between neurons and blood vessels, thus they are enabled to transmit signals that regulate blood flows in response to neurons activity. The importance of astrocytes as mediators of BBB formation and function has been shown in transplantation studies, investigating the ability of purified astrocytes to induce barrier properties in non-CNS blood vessels [9], as well as in vitro cocultures, in which their abilities to induce barrier properties in cultured endothelial cells were assessed [2]. Most of the characteristics of the BBB (*i.e.* those concerning the regulation of macromolecules and ions movements between the luminal and abluminal compartments) are

mainly due to the presence of junctions holding CNS endothelial cells, choroid plexus epithelial cells and cells of the arachnoid epithelium together [1]. The junctional complexes between ECs consist of adherents junctions (AJs) and tight junctions (TJs). In AJs, cadherin proteins extend throughout the intercellular cleft, thus holding cells together and giving structural support to the tissue. They are essential for formation of tight junctions, and their disruption leads to barrier disruption. The TJs (Figure 2) consist of a further complex of proteins crossing the intercellular cleft (*i.e.* occluding and claudins), and junctional adhesion molecules (JAMs) [10]. Works on ECs have shown that the abovementioned cellular adhesions generate on the apical part of the lateral membrane by interactions of transmembrane molecules connected to the cytoskeleton by means of cytoplasmic adaptors (*e.g.* ZO-1, ZO-2 and ZO-3), and that the strength of the junctions varies depending on the tissue [11]. Particular tight junctions called *zonae occludentes* are a fundamental characteristic of the BBB: they highly reduce permeation of polar solutes through paracellular diffusional pathways. The reduced ion movement results in the high *in vivo* transendothelial electrical resistance of the BBB of $\sim$1800 $\Omega \cdot cm^2$, showing the high effectiveness of the tight junctions in impeding this pathway [12].

Given the above, the main functions of the blood-brain barrier can be summarized as follows. The BBB:

- Maintains a controlled composition of ions that result optimal for synaptic signalling, through the combined effect of ion channels and specific transporters
- Keeps neurotransmitter pools of central and peripheral nervous systems separate, in order to avoid "crosstalk" and prevent neurotoxic damage due to uncontrolled levels of transmitters being released into the brain interstitial fluid (*e.g.* glutamate)
- Prevents potentially dangerous macromolecules from entering the brain (e.g. large molecular weight plasma proteins) and other neurotoxic substances circulating in the blood

- Cooperates to brain nutrition allowing the passage of many essential water-soluble nutrients and metabolites needed by nervous tissue, thanks to a low passive permeability towards those substances and specific transport systems

1.2.2 Transport across the BBB

Efficient drug delivery to the neural tissue of CNS across the blood-brain barrier remains a major challenge for the treatment of brain diseases, because of BBB's low permeability and the presence of active efflux transporters [13]. The ways in which substances travel from blood stream towards the cells composing living tissues can be categorized in two distinguished routes:

- Paracellular pathway, in which substances travel from the blood through the intercellular cleft of endothelial cells
- Transcellular pathway, in which substances travel through and within the cells themselves

According to De Bock *et al.* (2016): "As the highly sophisticated, interendothelial junctional complex efficiently impedes the random influx and efflux of molecules by paracellular diffusion, exchange between the blood and nervous system parenchyma is largely dependent on specific transport systems that mediate selective entry and removal of nutrients, inorganic ions, regulatory factors, and toxic waste products, respectively. This selective transport across the BBB, mediated by carriers and receptors, forms an essential and well-defined aspect of the barrier function of brain capillary endothelial cells." That is, the prominent route of transport for substances across the BBB is the transcellular pathway, namely transcytosis.

Transcytosis describes the endocytosis of cargo-loaded vesicles at the membrane on one side of the cell, their migration through cell cytoplasm, and the fusion of the vesicles with target membrane with the release of their content into the extracellular space. Endocytosis refers to the series of processes concerning the cellular internalization of substances from the extracellular environment. The different mechanisms of endocytosis can be grouped into clathrin-dependant and clathrin-independent. The first kind occurs at clathrin-coated pits, which are invaginations found on the

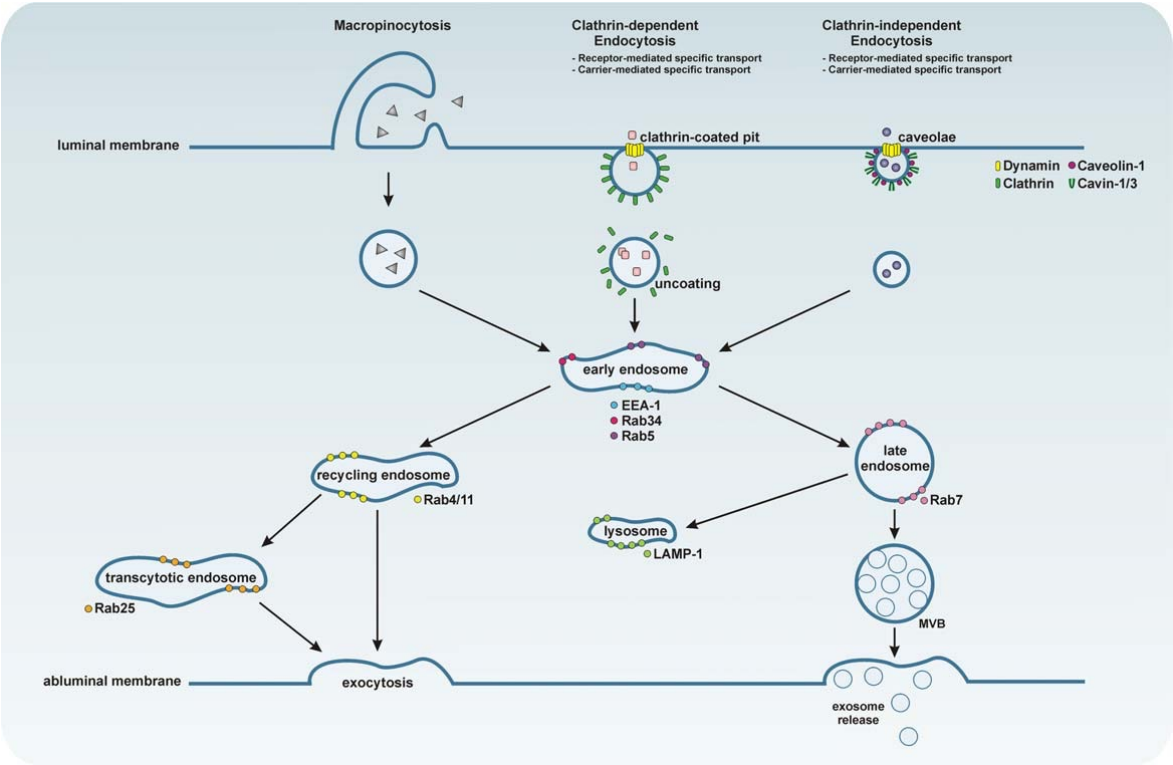

Figure 3. *Basic concepts of transcytosis. All these endocytosis pathways ultimately generate cytoplasmic vesicles that release their cargo at the opposite membrane via recycling/transcytotic endosomes or extracellular vesicles (exosomes), or to degrade their content by fusing with the lysosomal compartment [14].*

plasma membranes in almost every eukaryotic cell [14]. The main vesicles responsible for clathrin-independent mechanisms are caveolae pits and macropinocytotic vesicles. Caveolae are specialized membrane buds, made of cholesterol and sphingolipids, which generate uncoated vesicles [15]. In micropinocytosis, large amounts of extracellular fluid and molecules are internalized through the formation of actin filaments upon the plasma membrane that close on themselves and fuse with the underlying membrane itself. This way, solutes and soluble substances are trapped in the newly formed vesicle; the process is therefore called fluid-phase endocytosis. After endocytosis occurs, cargo-packed vesicles are transported through cell cytoplasm, sorted by early endosomes, and eventually fuse with target membrane releasing their content into the extracellular compartment [14]. The basic concepts of transcytosis are summarized in Figure 3.

Focusing on what happens specifically at the BBB, there is a directionality of compound transport that depends on the energy requirement of the mechanisms. Directionality of energy-independent transports is ruled by the concentration gradients of the substance, while energy-dependent mechanisms may act in both direction according to the distribution of transport proteins [16]. Small molecules are transported by specific carriers that can be either energy-dependent or -independent. On the other hand, essential macromolecules are carried across the BBB via specific energy-requiring receptors found on the luminal surface of endothelial cells [17]. After the creation of the bond between ligand and receptor, the complex is internalized by endocytosis, and the vesicle migrate through the cytoplasm towards the abluminal side of the cell. Here, the vesicle fuse with the membrane, completing a process that is commonly referred to as receptor-mediated endocytosis (RMT) [18]. This process primarily occurs at clathrin-coated pits and, since those pits are mostly found on the luminal membrane, the RMT occurs mainly in the blood-to-brain direction [19]. Alternative methods that allows crossing the BBB are: passive diffusion, fluid-phase endocytosis (macropinocytosis), non-specific adsorptive transcytosis and cell-mediated transcytosis. A limited number of small molecules and peptides can penetrate the BBB by passive diffusion, while larger hydrophilic molecules need fluid-phase endocytosis or adsorptive endocytosis to occur in order to access the brain. While the latter requires an electrostatic interaction between molecules and membrane, the former is achieved by engulfing extracellular fluid (with dissolved solutes) and thus does not require any molecule-membrane interaction [14]. It was recently discovered that in cell-mediated endocytosis immune cells (*e.g.* monocytes or macrophages) can cross the BBB transporting different types of molecules, thus representing a potential route for drug transport [20].

Given the above, the BBB makes difficult the development of new treatments of brain diseases. The majority of drugs used today in clinical practice for brain treatments exploit lipid-mediated passive diffusion across the BBB. To do so, drugs need to satisfy two criteria, have a molecular weight MW<400 Da and a high lipid solubility. Knowing this, small molecules drugs destined to brain

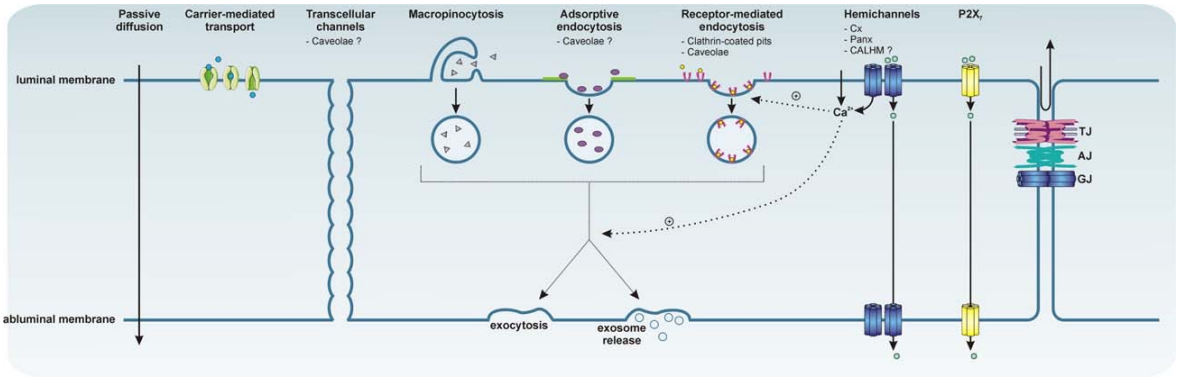

Figure 4. *Transcellular transport across the blood–brain barrier. Alternatively to paracellular diffusion, different modes of transcellular passage have been described at the level of the cerebral capillary endothelial cells that constitute the BBB. These include (i) free, passive diffusion limited to a select set of lipophilic small compounds, (ii) carrier-mediated transport, and (iii) transcellular events mediated by vesicles.*

treatments can be engineered to satisfy these requests (*e.g.* water soluble drugs can be modified into lipophilic compounds by blocking hydrogen bond forming functional groups on the molecule itself) [13]. On the other hand, large molecule drugs can be delivered across the BBB through alternative approaches. One of these methods exploits the endogenous carrier-mediated transcytosis (CMT) systems within the BBB; specifically it consists on modifying the structure of the drug in order to increase its affinity for one of carrier-mediated BBB transporters [21]. With the same approach, the presence of receptor-mediated transcytosis systems (RMT) enables the reengineering of proteins, making them BBB-penetrating drugs exploiting MTH technology (*i.e.* MTH is a peptide that cross the BBB on a specific RMT system) [22]. Finally, biodegradable polymeric nanoparticles have been proved to carry several drugs across the BBB, by modification of their surface (*e.g.* with PEG) to enable their entry into the brain via RMT [23].

The transcellular transport across the blood-brain barrier is summarized in Figure 4.

1.3 Models of the BBB

Due to BBB protection, inside the brain parenchyma most of drugs meant to treat CNS disorders are unable to gather in concentrations that would be therapeutically relevant. On the other hand, drugs meant to act in peripheral areas should be prevented from reaching the brain parenchyma in order to avoid cytotoxicity [24]. *In vivo* testing is not suitable for the early steps of drug discovery, even though those techniques are among the most accurate approaches to estimate BBB permeability of drug candidates. Moreover, these models show differential expression of enzymes, transporters and junctional proteins from those found in humans [25]. Given the above, in order to evaluate drug transport more precisely and to reduce attrition in later stages of drug development process, it would be better to carry out toxicity and permeability analysis not on human *in vivo* models, but on *in vitro* ones [24].

1.3.1 In vitro models

In vitro models of the blood-brain barrier are fundamental tools in studies concerning BBB development, physiology, pathophysiology, toxicology and the development of brain-penetrating drugs [24]. The first known efforts to generate cell cultures of CNS endothelial cells date back to early 1970s, due to the successful work of Joo and Karnushina on the isolation of brain capillaries [25]. From those first results, several different studies have been carried on with the purpose of developing a model that will show the most important *in vivo* characteristics of the BBB, at the same time being simple and economical enough to be efficiently implemented in high-throughput pharmaceutical research [26].

In order to reproduce the BBB characteristics in vitro, the simplest approach is to isolate and cultivate CNS endothelial cells in 2D cultures: ECs are seeded on a semipermeable membrane forming a uniform layer and studies on drug transport can be performed, depending on the pore size of the filter. The cells used can be from primary or immortalised lines, from any animal species [27]. The major downsides of this first model is the lack of interactions between ECs and other cells

composing NVU, and poor barrier properties showed. Hence, the most used *in vitro* models of the BBB are co-culture systems [26].

Since the work of Janzer and Raff published in 1987 demonstrated that astrocytes could induce tight junction properties in endothelial cells similar to values observed in *in vivo* BBBs, astrocytes have been extensively implemented in co-culture *in vitro* models [28]. The result was a significant improvement of paracellular barrier properties compared to mono-culture models [29]. With regard to other cellular components of the NVU, like pericytes, studies related to their influence within this kind of systems are rare. For pericytes, one reason for this lack of publications could be the absence of specific PCs markers [30]. On the other hand, the fundamental role of neurons in regulating BBB permeability leads to an enhanced use of these cells in tri-culture models setup. In this particular type of co-culture models, the influence of neurons (or glia) and astrocytes on endothelial cells permeability is analysed [31]. Despite co-culture models are the favourite choice amongst *in vitro* BBB models, a significant number of such models have shown suboptimal results (*e.g.* low TEER values and high paracellular permeability) [26].

Focusing on human cell-based models, they are mostly used to translate therapies to humans, since there are differences between human and other species among transporter genotypes. The main issue with human models is the absence of a reliable source of cells, and the approaches to this problem are mainly two: immortalised cell lines and stem cells. It would be ideal to use primary human endothelial cells but, due to ethic restrictions, to date only a few lines of immortalised cell have been identified to generate *in vitro* models of the BBB [32]. Moreover, immortalised cell lines show inferior TEER values with respect to an *in vivo* environment, demonstrating to be unable to form a fully functional barrier even under optimized culture conditions [33]. On the other hand, human stem cells are the best source of brain-like endothelial cells in large scales, obtained by differentiation of human pluripotent stem cells [34]. They have shown strong barrier functions (TEER= 1450 ± 140 $\Omega \cdot cm^2$) under co-culture conditions. However, the differentiation process is complex and the values of TEER started to decrease after 50 hours of culture [35].

Finally, the last typology of models analysed are 3D dynamic models. These shows the advantage, when compared to 2D models, to control and analyse the effects of confinement, geometry and flow conditions on cell behaviour. 3D models are able to generate high TEERs with human cells, but their drawbacks (*i.e.* large amounts of cells needed, difficulties in obtaining a real-time monitoring, and the technical skills required to setup the model) make it inappropriate for high-throughput pharmaceutical screening [36]. A possible solution are microfluidic devices, which uses small fluid volumes and therefore requires fewer cells, and permit visualisation of cells thanks to the use of transparent materials. Marino *et al.* [38] designed and realized a dynamic 3D biohybrid model of the BBB able to reproduce the microvasculature structure of the neurovascular system on a 1:1 scale. Microtubes were fabricated to mimic brain capillaries using two-photon lithography (TPL) and then employed as substrates for the co-culture of bEnd.3 and U87 glioblastoma ECs. The cultures exhibited the maturation of TJs, good results in terms permeability to dextran and a reliable TEER value, therefore showing a good mimicking of the physiological BBB.

Given the above, according to Banerjee *et al.* "a model that can be recognized as the gold standard for predictable high-throughput screening application has not yet been reported" [26].

1.3.2 In vivo models

Despite selective utility of *in vitro* blood-brain barrier models, no *in vitro* model is able to fully reproduce the BBB as found in *in vivo* examples. Therefore, an *in vivo* BBB model is needed to be able to provide the most reliable evaluations and characterizations of BBB-penetrating drugs [38]. Since the methodologies exploited in *in vivo* environments show low throughput screening capacity, they are mostly used in advanced steps of drug development researches. However, the importance of results obtained *in vivo* for optimization and validation of *in vitro* models is undeniable [39]. Several models have been developed, each with its own advantages and disadvantages. Currently, the most used *in vivo* animal models are mice, because several key features (*i.e.* cell types, transporters and permeability properties) are very similar to those found in

the human BBB [7]. These models are mainly used to estimate the ability of drugs to overpass the BBB, by asserting the rate of permeation and of brain penetration of a substance across the barrier [1]. The extent of brain penetration is studied in rodents and is calculated under steady-state conditions as the ratio (or the logarithm of the ratio) of total brain and plasma concentrations [40]. The values are obtained from plasma and brain at different time steps after an interperitoneal, intravenous, oral or subcutaneous administration of the compound [38]. On the other hand, the rate of permeation is determined through the brain uptake index technique, the *in situ* brain perfusion method, the intravenous injection technique, intracerebral microdialysis and non-invasive techniques [39]. The procedures are described below.

In the *in situ* brain perfusion, a catheterization of the external carotid artery of the animal is performed. All branches of both external and internal carotid are then ligated, and the substances are perfused into the internal artery. After the decapitation of the animal and the collection of the brain, the reference and test compounds are quantified. This technique allows the study of different characteristics of drug transport across the BBB but does not measure free drugs concentration inside the brain and is time and money consuming [39].

In the brain uptake index technique, a bolus injection of radiolabelled test and reference compounds is performed in the common carotid artery of an animal. Decapitation occurs after 5-15 s to avoid brain efflux, and then brain concentrations of compounds are determined and related to plasma ones to calculate the index. It is a fast and flexible technique, since it allows adjustments of the injected composition. However, since the brain is shortly exposed to the compound, it is impossible to study slow uptake mechanisms with this technique [41].

To perform intracerebral microdialysis, the insertion of into a specific area of the brain is performed and the area is then perfused with a physiological solution whose ionic composition is similar to the extracellular cerebral fluid's one. The dialysis liquid is collected at different time steps in order to measure the compound free concentration. Although this technique allows the determination of

unbound drugs concentration in different brain areas and requires a reduced number of animal subjects, it is expensive and low throughput [42].

To evaluate the brain efflux index, the test and reference compounds are directly injected into the brain. After decapitation, the brain is collected, and the concentrations of the substances are measured at defined time points. The advantage of this approach is that it allows an evaluation of the efflux transporters influence in the passage through the barrier. On the other hand, the injection procedure may modify BBB properties and needs large numbers of animals [43].

The aforementioned techniques are categorized as invasive. Non-invasive procedures (*e.g.* MRI, PET, SPECT) are useful to evaluate the permeability of the BBB, perform transport studies, analyse the function of efflux transporters and validating *in vitro* results. However, they are expensive and incompatible with routine screening [38, 41].

Finally, a particular type of *in vivo* models are the so called "model organisms". The attractiveness of model organisms is that the screening process can be performed using a functional read-out of the whole organism, based on toxicity, behaviour or pharmacodynamics. Among all, *Drosophila* and zebrafish are the most used for BBB research [44]. In *Drosophila*, some features of the single epithelial layer barrier surrounding brain (*e.g.* mechanisms of chemicals efflux) make the model useful in screening efflux pump substrate and their toxicity. Unfortunately, the differences between species in cellular and structural aspects limit the applicability of this model [45]. In contrast, the BBB in zebrafish shows remarkable similarities to that of mammals [46]. This model organism has been used recently for *in vivo* screening of BBB permeability [47]. Moreover, genetic manipulation of zebrafish is relatively easy and has been employed to produce CNS "disease-like" models [48]. However, the reliability of these results concerning their translation to higher species is yet to be asserted [44].

1.3.3 Applications

The existence of a blood-brain barrier gives raise to difficulties in delivering therapeutical molecules to the brain, therefore making the treatment of CNS disorders a great challenge. Several approaches have been shown to improve brain drug delivery, namely:

- BBB temporary disruption, which causes an increase in brain capillaries permeability through biological, physical or chemical stimuli [50].
- Chemical drug modification, which provides that the hydrophilic structure of the drug is masked to increase its lipophilic properties, and, therefore, to improve its transport [51].
- Drug conjugation, which exploits natural or artificial ligands to improve molecules interactions with influx transporters [52].
- Nanoscale drug delivery systems (*e.g.* liposomes, micelles, nanoparticles), which allow a highly specific drugs transport across the barrier often due to ligands placed on their surface [53].

Both *in vitro* and *in vivo* BBB models can be used to assess the efficacy of the aforementioned approaches. In this context, in vitro models of the BBB are usually employed to estimate the processes of cellular uptake, the internalization trends of the nanocarriers, their toxicity and ability to cross cell layers [40]. For example, Rempe *et al.* [54] used an *in vitro* porcine model to assess the TEER and the permeability of paracellular markers of a BBB under the effect of nanoparticles made of poly(n-butylcyano-acrylate). Conclusions obtained from *in vitro* studies need to be confirmed *in vivo*. The intravenous injection method is the most used *in vivo* model for assessing pharmacokinetics and distribution of nanocarriers. The results obtained *in vivo* are usually consistent with those *in vitro*, demonstrating that both kinds of models are needed to fully characterize brain drug delivery systems [40].

1.4 Electrospinning

Electrospinning started to be recognized as an appropriate technique to spin small-diameter fibers after 1934, when Formhals patented the process. The first result he obtained was to successfully spin cellulose acetate fibers using an acetone/alcohol solution [55]. In the years that followed, scientists worked on obtaining a better understanding of the underlying process. The most relevant was in 1969, when Taylor published his work investigating how the droplet of polymer at the end of the tip reacts under the effect of an electric field [56]. Over the last two decades, the electrospinning technique has proved promising for many applications, mainly due to the cost- and time-effective production of high-surface-to-volume fibrous structures [57].

1.4.1 Technology, materials and applications

The process of electrospinning utilizes electrostatic forces to generate continuous polymer fibers, (with fiber diameters varying from micrometres to nanometres) from polymer melt or solution. It is performed at room temperature and atmospheric pressure, with vertical or horizontal arrangement. A typical electrospinning setup (Figure 5) is composed of:

- A syringe (needle tip)
- A high voltage power supply (electric field) with positive or negative polarity
- A grounded fiber collector

The liquid to be electrospun is forced through a small-diameter capillary by a syringe pump, gravitational forces or pressurized gas, and forms a droplet at the tip. The basic idea of electrospinning is to apply high voltage on the polymer solution strong enough to overcome polymers surface tension and induce fiber formation. An electrode from the power supply is therefore inserted within the melt or can be directly placed onto the metal needle, if used. Induced by charge injected into the solution, the electric field (directed from the tip to the collector) induces surface charge repulsion of solution which force the spherical drop into conical shape (Taylor's

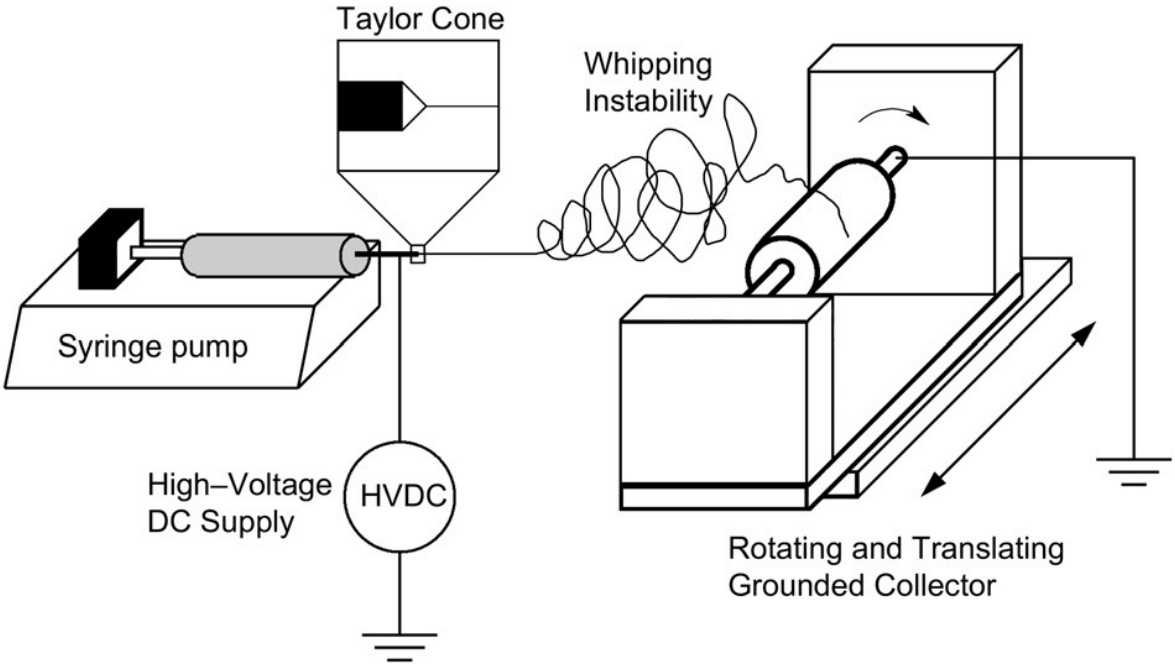

Figure 5. *Setup of a typical electrospinning apparatus.*

cone). As the electric field is increased, electrostatic forces overcome polymer surface tension. Consequently, a fiber jet ejects from Taylor's cone and is accelerated toward the grounded collector. Simultaneously, fibers accelerated through the atmosphere undergo a chaotic bending instability which aid the solvent evaporation process. Finally, dried fibers are found on the collector. Different configurations for the collector configurations can be used. For example, a stationary collector is used to obtain a randomly oriented fiber mat, while the use of a rotating collector will result in the formation of an aligned fiber mat [55, 56].

Fiber formation and structure depend on a number of parameters that can be classified into:

- Solution parameters (polymer concentration, solvent volatility, solution conductivity)
- Processing parameters (applied voltage, flow rate, capillary-collector distance)
- Ambient parameters (temperature, humidity, air flow)

The polymer concentration determines whether a fiber forms or not (spinnability). Lower polymer concentrations lead to the formation of beads within the fibers. Higher polymer concentrations increase fiber diameter and could eventually prevent jet ejection. Thus, a defined range of polymer concentrations exists in which fibers can be successfully electrospun [57].

The choice of solvent affects the spinnability, and influences fiber porosity as well. A volatile solvent must be used in order for solvent evaporation during the flight between the cone and the collector to happen, due to a phase separation [58].

Solution conductivity influences fiber size. Higher conductivity means that the solution has a greater capacity for carrying charges. Thus, the fiber jet will be subjected to a greater tensile force (the radius of the jet is inversely related to the cube root of the conductivity) resulting in bending instability and a broad diameter distribution [59].

Flow rate of polymer solution and applied voltage are correlated. Both fiber diameter and pore size are directly related to flow rate, and, additionally, greater feeding rate results in the formation of more bead defects, due to the inability of solvent to fully evaporate before fibers can reach the collector [58]. A higher voltage applied could prevent the formation of beads, but consequently would cause non-uniform diameter distribution and uncompleted solvent evaporation. Lower flow rate or voltage are responsible to failures in jet formation. Thus, there are optimized ranges of electric field strength and of flow rate for a certain polymer/solvent system [60].

Fiber size con also be influenced by the distance between capillary tip and collector and depends on concentration of the solution and applied voltage. A minimum distance is required to give the solvent enough time to evaporate before reaching the collector [61]. It has been shown that the fiber diameter is inversely related to the distance from the Taylor's cone [62].

In order for electrospun fibers to be exploited in tissue engineering applications several considerations must be taken into account (*e.g.* choice of material, fiber orientation, porosity, surface modifications and tissue application). A candidate material for TE first of all must be biocompatible [56]. To date numerous biopolymers, biocopolymers and biopolymer blends have been investigated to assess their potential for electrospun scaffold fabrication: poly(lactic acid) (PLA) and its stereoisomers, poly(glycolic acid) (PGA), copolymer poly(lactic-co-glycolic acid) (PLGA), poly(ε-caprolactone) (PCL), chitosan, collagen, gelatine, polyvinyl alcohol (PVA) poly(ethylene oxide) (PEO) and poly(ethylene glycol) (PEG) have been the most commonly used [63]. Current

studies have focused on the incorporation of compounds showing bioactivity to influence and manipulate the biological environment due to surface modifications [64].

Focusing on applications, electrospinning has been exploited for a number of tissues in the field of TE. Thanks to the possibility to realize aligned scaffolds, tune mechanical and biological properties and prevent cell migration, electrospinning has seen a great use in the area of tissue engineered grafts for blood vessels. Inoguchi *et al.* [65] developed poly(L-lactide-co-ε-caprolactone) tubular scaffolds able to mimic mature arteries response to pulsatile flows, as well as promote endothelial cells attachment.

Electrospun fibers have shown to be promising to make scaffolds for another tissue: bone. Nie and Wang [66] observed that encapsulation of DNA/chitosan in PLGA/Hydroxyl apatite (HAp) electrospun scaffolds has the potential to augment bone tissue regeneration, due to the effect of HAp in enhancing encapsulation efficiency and DNA release.

Electrospinning has also been investigated for neural tissue engineering applications. For example, Yang *et al.* [67] assessed the effect of aligned and random scaffolds made of electrospun PLLA fibers on the morphology and activity of neural stem cells.

One final area where electrospinning has been successfully employed is the fabrication of scaffolds for tendon and ligament repair, as seen in works such as the one of Ouyang *et al.* [68] showing the effect of PLGA scaffolds in tendon regeneration.

The electrospinning process has also been proven to be a reliable fabrication technique for drug delivery systems. The most important aim when developing a drug delivery system is the design of drug release and degradation rate of polymer. To date, a number of drugs have been used in electrospun DDS (e.g. antibiotics, anticancer drugs, proteins, DNA) [56]. Drug loading can be performed by several methods: post-spinning modifications, electrospinning of drug/polymer or polymer/nanoparticle blends, emulsion electrospinning and core-shell electrospinning by co-axial setup [55]. On the other hand, as shown by Park *et al.*, porous composite fibers realized through co-axial electrospinning can help control drug release [69].

1.4.2 Electrospun cellulose bio-interfaces

Cellulose acetate (CA) is a synthetic compound defined as the acetate ester of cellulose. Cellulose is a natural polymer, made up of recurring units, with the following molecular structure.

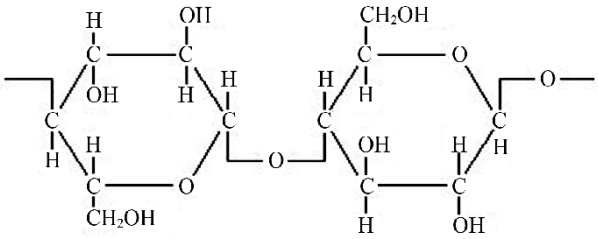

Cellulose

CA is usually prepared (Figure 6) by mixing cellulose with acetic acid, acetic anhydride and a catalyst (*e.g.* sulfuric acid). The resulting product, known as primary cellulose acetate or cellulose triacetate, can further be treated with water to obtain secondary cellulose acetate, or cellulose diacetate. After formation, CA is dissolved in acetone, forming a viscous solution for extrusion [72].

The simple and high effective technique of electrospinning has given new perspectives to the application of CA fibers [73]. In the realm of biotechnology, electrospun CA fibers have found a spectrum of applications across different domains (Figure 7). The more prominent uses are immobilization of biomolecules, TE, biosensing, nutraceutical delivery, bioremediation and the development of antimicrobial mats [74].

First of all, electrospun CA nanofibers are interesting as immobilization matrix for a number of bioactive molecules (*e.g.* biocatalysts, polysaccharides, cytokines, anticancer drugs). For example, vitamin A and vitamin E have been successfully immobilized onto electrospun CA nanofibers showing a more gradual release compared to cellulose films [75]. Enzymes have been immobilized as well, showing almost the same activity as in their free state and even an increased durability [76]. In the field of drug loading, different studies have recently focused on the use of electrospun CA fibers to develop transdermal drug delivery systems [74]. This method of drug administration ensures a

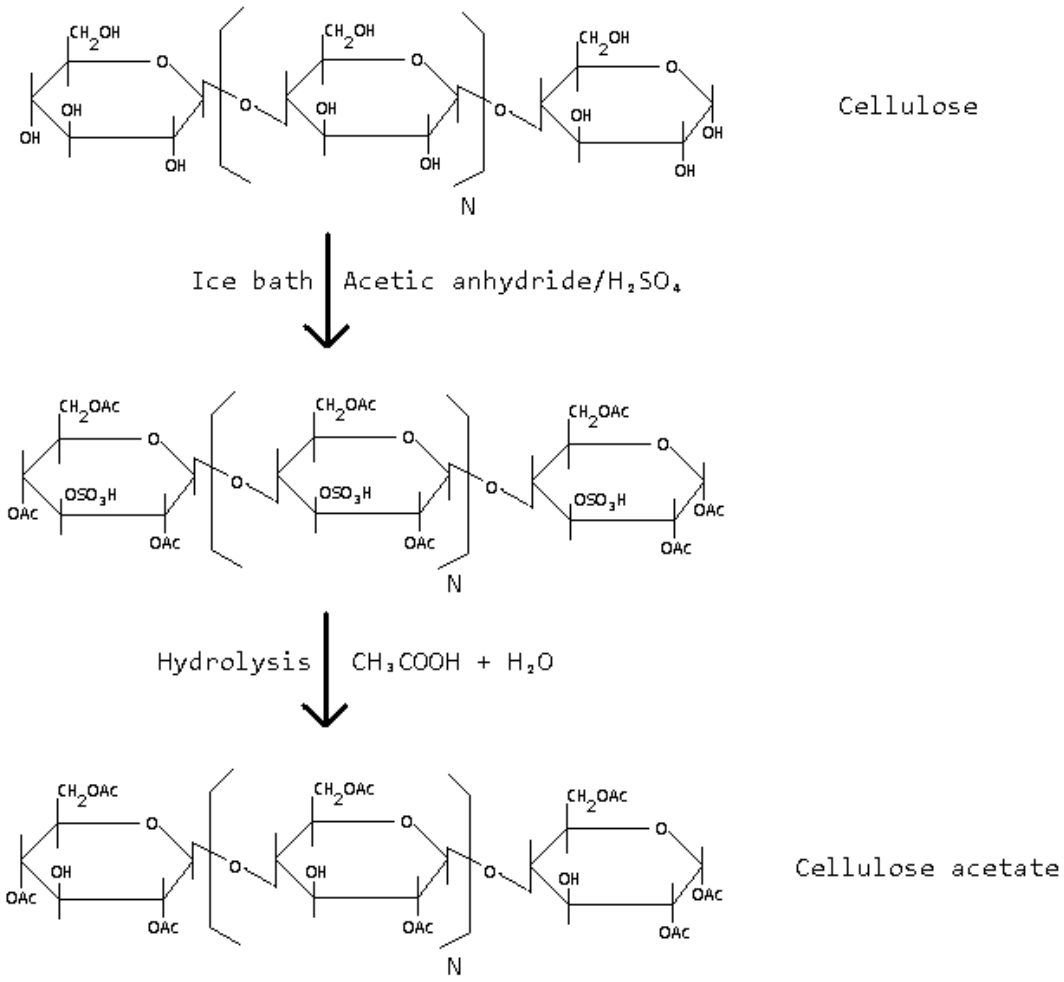

Figure 6. *Preparation of cellulose acetate [72].*

predetermined and controlled release and has proved to improve compliance and reduce variability both inter- and intra-patients. One last application is the use of bioconjugated CA fibers for crop protection and insect control, through the immobilization of insecticides, repellents and even pheromones [77].

In the field of tissue engineering, electrospinning is an effective method to generate cellulose based fibrous scaffolds, even though more studies need to be carried out in the field of TE-applied CA nanofibers. However, Rodriguez *et al.* [78] obtained scaffolds for bone healing through CA mats saponification. Rubenstein *et al.* [79] showed enhanced growth, adhesion and migration of human umbilical vein endothelial cells cultured on electrospun CA/chitosan scaffolds. And,

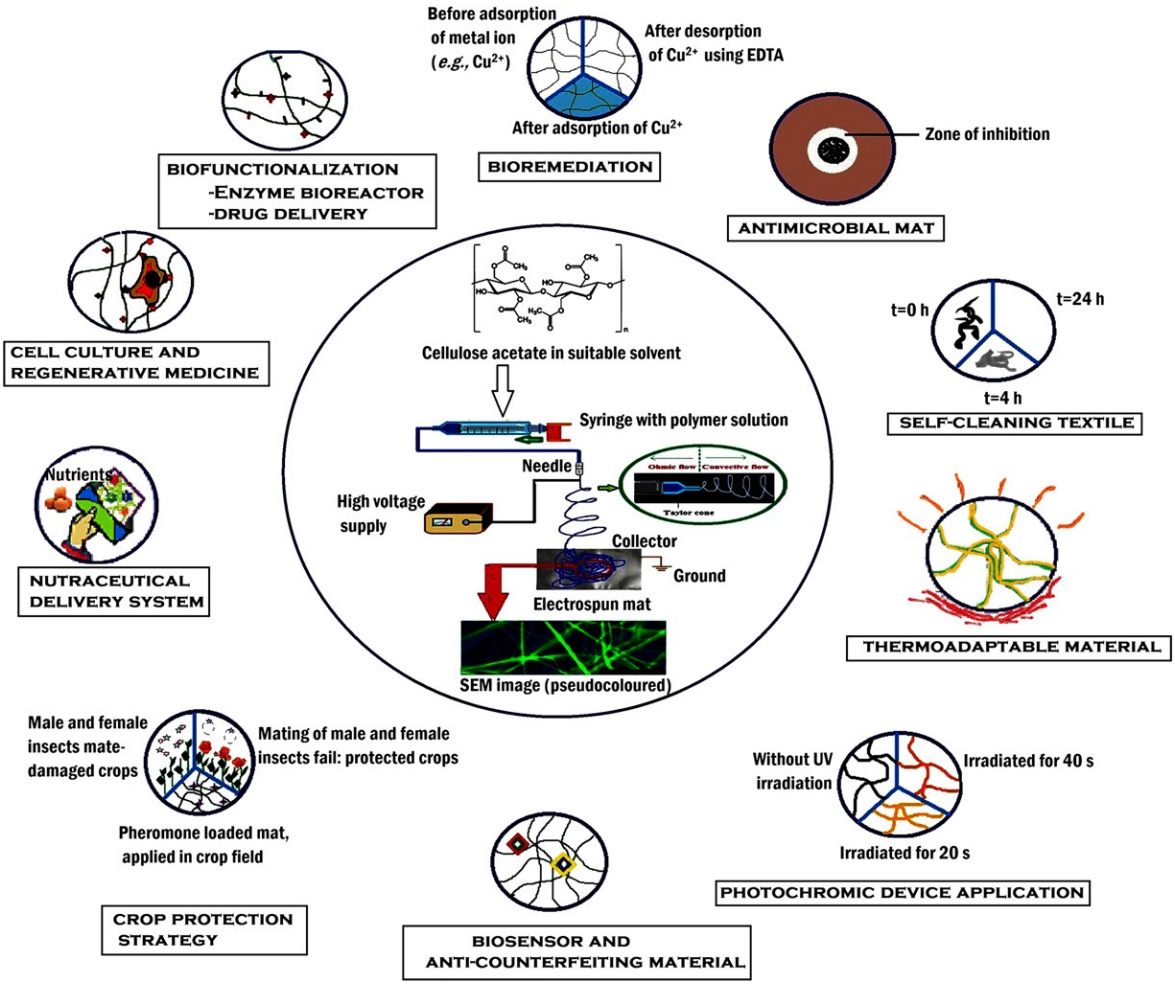

Figure 7. *Schematic representation of electrospinning cellulose acetate nanofibers (at the center) and myriad of biotechnological applications, the most preminent of which are presented in the text [74].*

finally, Eichhorn *et al.* [80] reported the growth of Schwann cells on aligned cellulose acetate butyrate nanofibers, opening new routes for neural repair.

Certain food ingredients also have a physiological role, and the protection of these bioactive components during storage is crucial [81]. Recently, electrospun CA nanofibers have been successfully employed in the preparation of edible mats. With nanoencapsulation, it is ensured the protection of nutrients and also their controlled release in the applications of nutraceutical delivery [82].

Another application for CA is biosensors. As shown by Wang *et al.* [83], electrospun CA fibers, having a high surface-area-to-volume ratio, can be used as a good platform to localize and immobilize sensing elements, also ensuring a proper exposure to the quenches.

Electrospun composite nanofiber structures are creating interest in a number of sectors in that are able to carry uniformly dispersed antimicrobial agents. For example, nanobiocomposites of CA have been reported to be loaded with antimicrobials such as silver and zinc [84].

One final field of application is that of bioremediation. Since the importance of the issue of heavy-metal induced water pollution in the food chain, Tian *et al.* [85] have showed the use of electrospun CA membranes for heavy metal ion adsorption in water treatment to be an adequate approach. On the other hand, zero-valent ion nanoparticles, immobilized onto electrospun CA nanofibers, are considered cost-effective benign agent for decolorization of organic dyes in dyeing waste water [86].

2 Materials and Methods

2.1 Substrate preparation and characterization

First of all, in order to realize the substrates for the *in vitro* model of the blood-brain barrier, solutions of cellulose acetate with different concentration were prepared to be electrospun. Cellulose acetate powder (*Gibco*©) was mixed with acetone, resulting in solutions at 15 wt%, 16 wt%, 17 wt% and 18 wt%. The solutions were then mixed through shaking and left to rest for 24 h in order to obtain a good level of homogeneity.

The setup for the electrospinning process was as follows. A 10 ml syringe (*Henke-Sass Wolf*©) with a 21G, 0.8x50 mm needle (*BD Microlance*©) was loaded with the liquid and placed into a programmable microfluidics syringe pump (NE-1002X, *ALA Scientific Instruments*©). The pump was programmed to dispense a flow rate of 1 ml/h. The electric field was generated by a power supply (*Linari Engineering*©), connected to both the syringe needle and the collector, through an applied voltage of 12 kV. The flat collector was covered with 2x2 cm squares of a stainless-steel woven wire mesh with 1 mm holes (Figure 8), in order for the spun membranes to be more easily manipulated afterwards, and the whole structure was positioned at 10 cm from the needle tip.

Membranes with different spinning times (*i.e.* 5, 10, 15, 20, 25 and 30 minutes) were eventually obtained, and images of them were taken through optical microscopy and SEM.

Another type of substrates was prepared starting from an 8 wt% cyanoacrylate (*Gibco*©) solution in acetone. The setup for the electrospinning process was the same as the one set for cellulose, except for the applied voltage of 10 kV. The substrates were all obtained with a spinning time of 1 min, due to the much faster deposition of cyanoacrylate fibers. In order to obtain not a fibrous membrane but a transparent and porous layer, a heating treatment followed the electrospinning step. The substrates were placed on a hotplate and heated at 150 °C for 20 seconds. Finally, images of the resulting items were taken with an optical microscope.

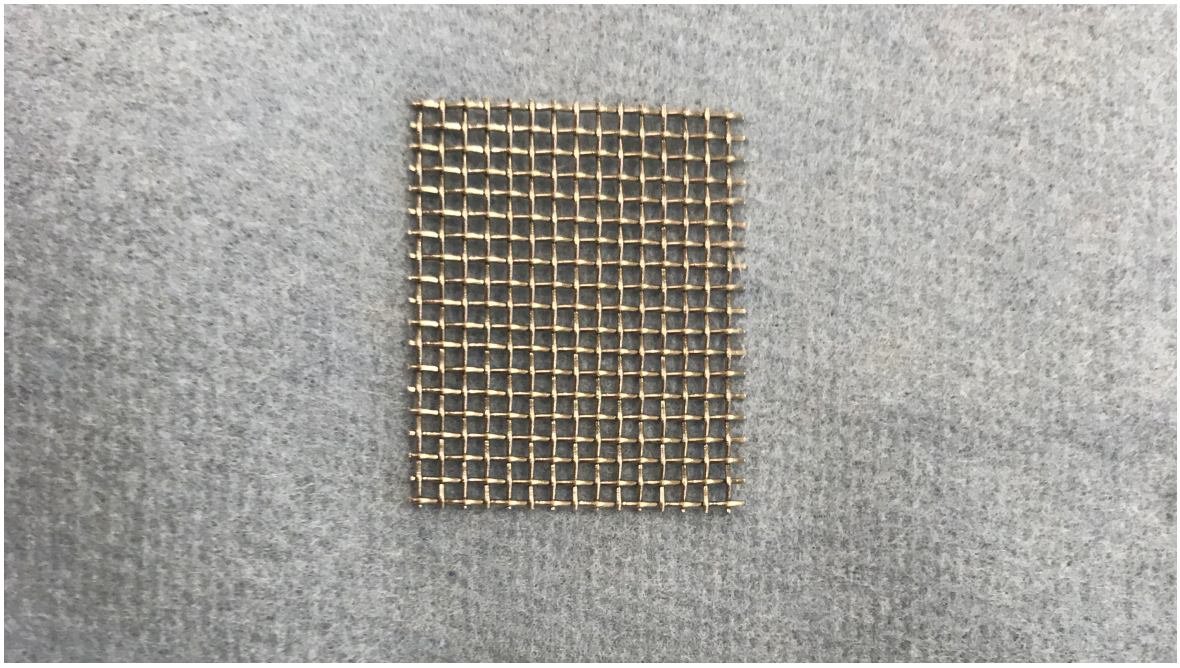

Figure 8. *Stainless-steel woven wire mesh with 1 mm holes used as support for electrospun membranes.*

However, for reasons explained in the results chapter, the cyanoacrylate substrates were eventually discarded, and the following steps were performed using only the cellulose acetate membranes.

2.2 BBB model preparation and characterization

2.2.1 Preparation of inserts for the in vitro model

To start, in order to obtain a suitable structure for the model, 3 µm porous polycarbonate Transwell® inserts (*Corning Incorporated®*) were used. The porous membrane was removed from the insert, and the glue residues were cleaned out of the structure through an acetone wash. The cellulose membranes were then placed on the insert with the flatter side (*i.e.* the one opposite to the metal grid) facing the interior of the insert. Polydimethylsiloxane (PDMS, *Gibco®*) was then used to fix the membranes to the side of the structures (Figure 9). The inserts were left to rest at 60 °C for 4 h to let the PDMS harden and then treated with UV rays for 24 h for sterilization.

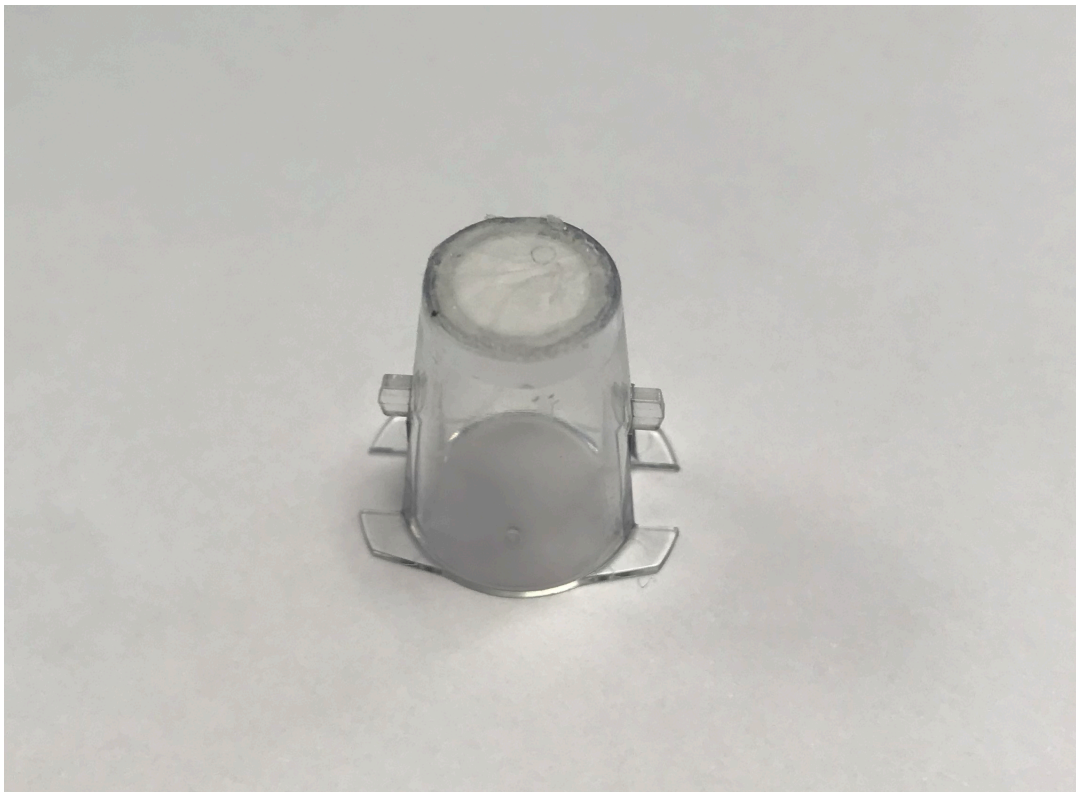

Figure 9. *Transwell insert with cellulose acetate membrane.*

2.2.2 Cell culture

Cultures of immortalized brain-derived endothelioma bEnd.3 cell line (*ATCC*® CRL-2299™) were performed in 75 mm^2 Petri dishes (*Corning Incorporated®*) using high-glucose Dulbecco Modified

Eagle's Medium (DMEM, *Sigma-Aldrich®*), supplemented with 10% fetal bovine serum (FBS, *Gibco®*), 1% sodium pyruvate, 1% L-glutamine, 1% pen/strep solution with 100 IU/ml of penicillin and 100 µg/ml of streptomycin (*Gibco®*). Cultures were maintained in a humified atmosphere (5% CO_2) at 37 °C.

1 h before seeding, the inserts were placed in a 24-well-plate (*Corning Incorporated®*) and incubated with the cell medium.

When the cultured cells reached a confluence of 90% inside the dishes, a trypsinization step was performed. Specifically, cells were treated with 2 ml of trypsin (*Gibco®*) for 5 minutes in a humified atmosphere (5% CO_2) at 37 °C; then 8 ml of medium was added and samples were centrifuged for 6 minutes at 23 °C with 2600. The cell pallets were then resuspended in trypsin-free medium for seeding.

The cells were eventually seeded at high confluence (seeding density $8 \cdot 10^4$ cells/cm^2) on the inner side of Transwell® filters, with a total final volume of 300 µl; 700 µl of medium was added on the external side of the Transwell® (Figure 10).

The cultures were maintained for 5 days, with medium replacements on day 2 and day 4.

2.2.3 Analysis of TEER and permeability

The model was characterized in terms of transendothelial electric resistance (TEER) and permeability.

The TEER was assessed using a Millipore Millicell ERS-2 Volt-Ohmmeter on day 2, 3 and 4 of the culture.

The permeability was assessed in terms of permeability to FITC-dextran (*Sigma-Aldrich©*) with a molecular weight of 4 kDa. Specifically, 100 µl of phenol red-free medium, containing 50 µg/mol of FITC-dextran, were added to the luminal compartments of the BBB models or of the inserts without cells, with the role of controls. The fluorescence emission of the medium in the abluminal compartments was measured with a Perkin Elmer Victor X3 UV-Vis spectrofluorometer (λ_{ex}=488

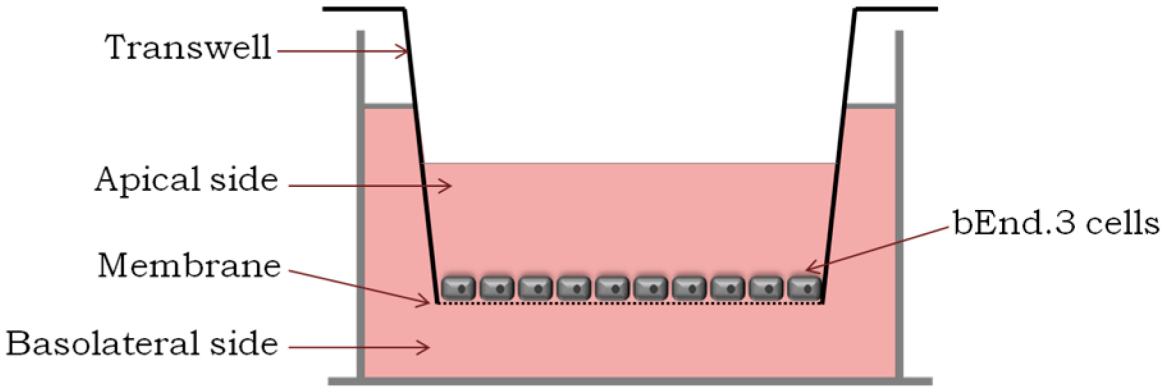

Figure 10. *Schematic representation of the BBB model using transwell insert.*

nm, λ_{em}=520 nm) at different time points (*i.e.* 10 min, 30 min, 4h). The values of fluorescence emission were converted and expressed in terms of FITC-dextran concentrations using a calibration curve.

2.2.4 Fixation, staining and imaging

In order to perform imaging, cultures were rinsed 3 times for 5 minutes in phosphate-buffered saline (PBS) and then were fixed using a paraformaldehyde (PFA) in PBS solution. Fixation in PFA was carried out by removing PBS from the wells, replacing it with 1 ml of 4% PFA, and then incubating the samples for 20 minutes at 4°C.

Thereafter, wells were extensively washed with PBS in order to remove PFA and the staining process was carried out through incubation with a staining solution of 1 ml of PBS, 1:100 goat serum, 1:1000 Hoechst dye (*Thermo Scientific*©) (*i.e.* a fluorescent stain specific for nuclei of eukaryotic cells) and 1:200 Phalloidin (*Abcam*©) (*i.e.* a fluorescent stain specific for f-actin filaments). The incubation was carried out for 1 hour 30 minutes at 37°C and, after a final wash, the staining solution was replaced with PBS and the wells were stored at 4°C.

Confocal laser scanning microscopy (CLSM) was performed using a C2s system (*Nikon*©) and image processing employed a NIS Elements software.

3 Results

3.1 Electrospun substrate characterization

Cellulose acetate electrospun membranes (Figure 11) were realized with different spinning times.

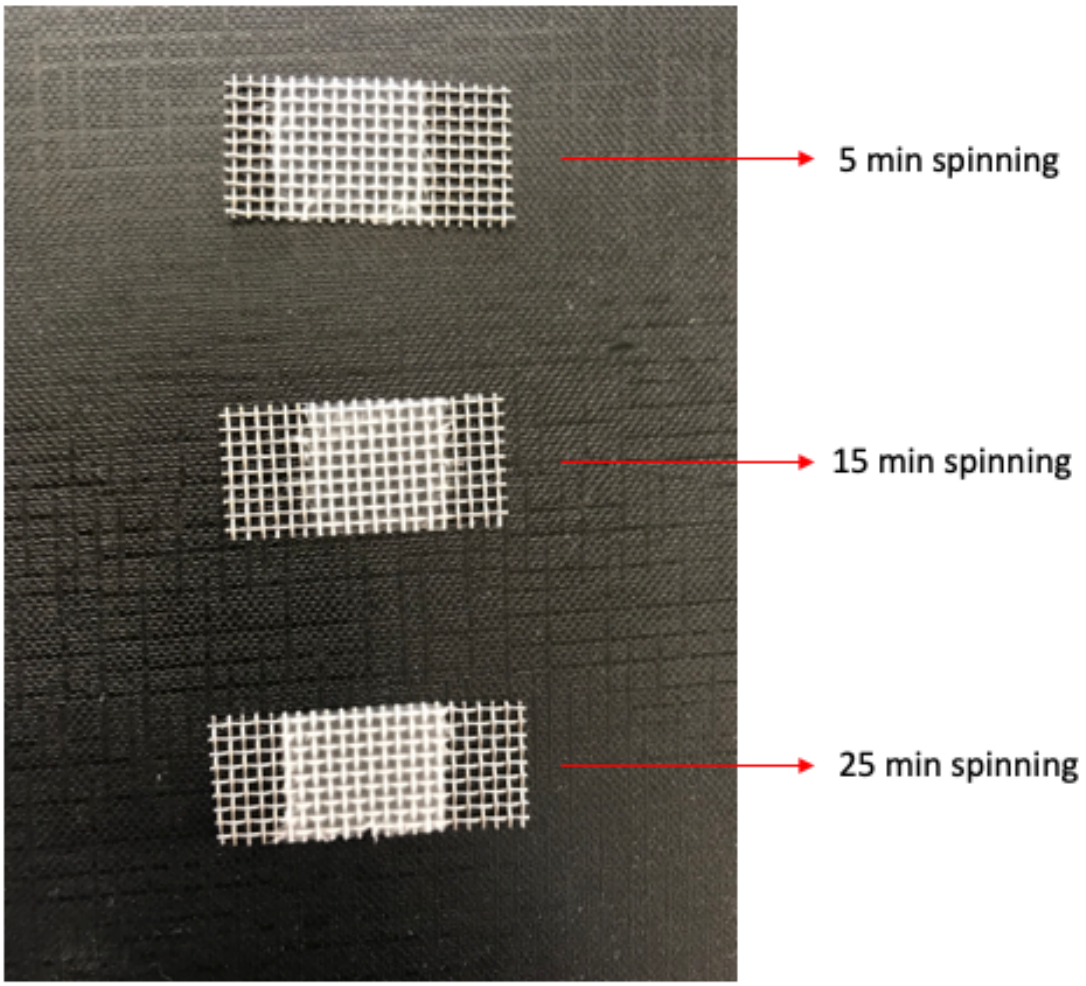

Figure 11. *Samples of cellulose acetate electrospun membranes on stainless-steel mesh.*

They were analyzed with optical microscopy and scanning electron microscopy (SEM). Figure 12 shows optical images of samples from different spinning times, while Figure 13 shows SEM images taken from the kind of sample that was actually used to realize the BBB model (*i.e.* the 25 minutes one). The presence of areas with higher opacity is due to the underlying metal grid: being an efficient electrical conductor, steel shows a significant accumulation of charges, when subjected to an electric field, that draw charged CA fibers towards the wire and away from the center of the square. Furthermore, there is a clear increase of fiber density on substrates with higher spinning

time, as expected. While this could be beneficial in so far as it determines a stronger structural integrity, on the other hand it could determine a loss in transparency, which could be detrimental for further analysis, if overstepped. On the other hand, SEM images show no signs of defects that typically affect electrospun fibers (*e.g.* beads, ribbons), indicating that process and solution parameters have been tuned properly.

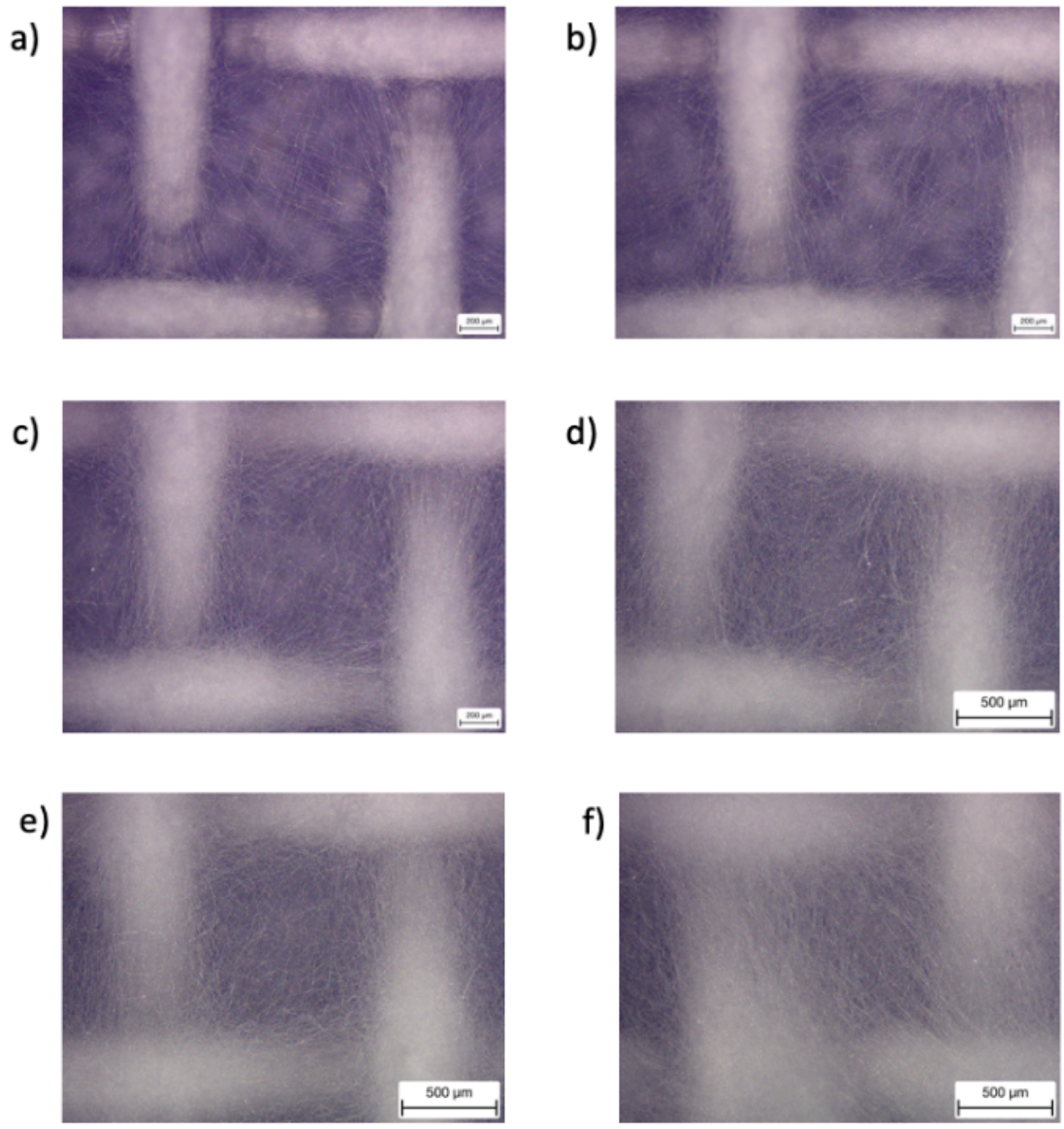

Figure 12. *Optical images of CA substrates after 5* ***(a)****, 10* ***(b)****, 15* ***(c)****, 20* ***(d)****, 25* ***(e)*** *and 30* ***(f)*** *minutes of spinning.*

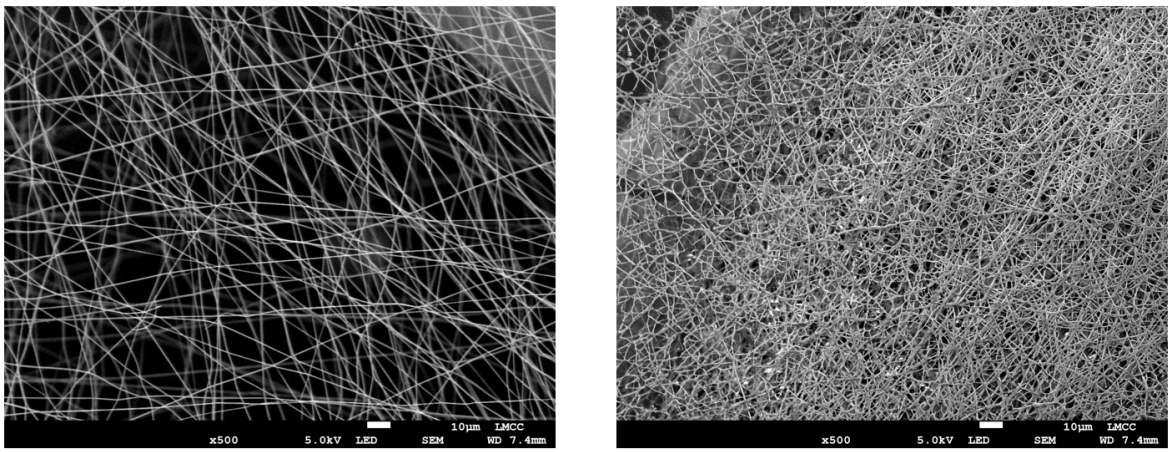

Figure 13. *Scanning electron microscopy (SEM) of cellulose acetate (CA) electrospun fibers in the area between the metal wires (left) and on the metal wire (right).*

Cyanoacrylate electrospun membranes were realized with a spinning time of ~1 minute and then subjected to a heat treatment (Figure 14). Optical images of both pre- and post-treatment samples are shown in Figure 15.

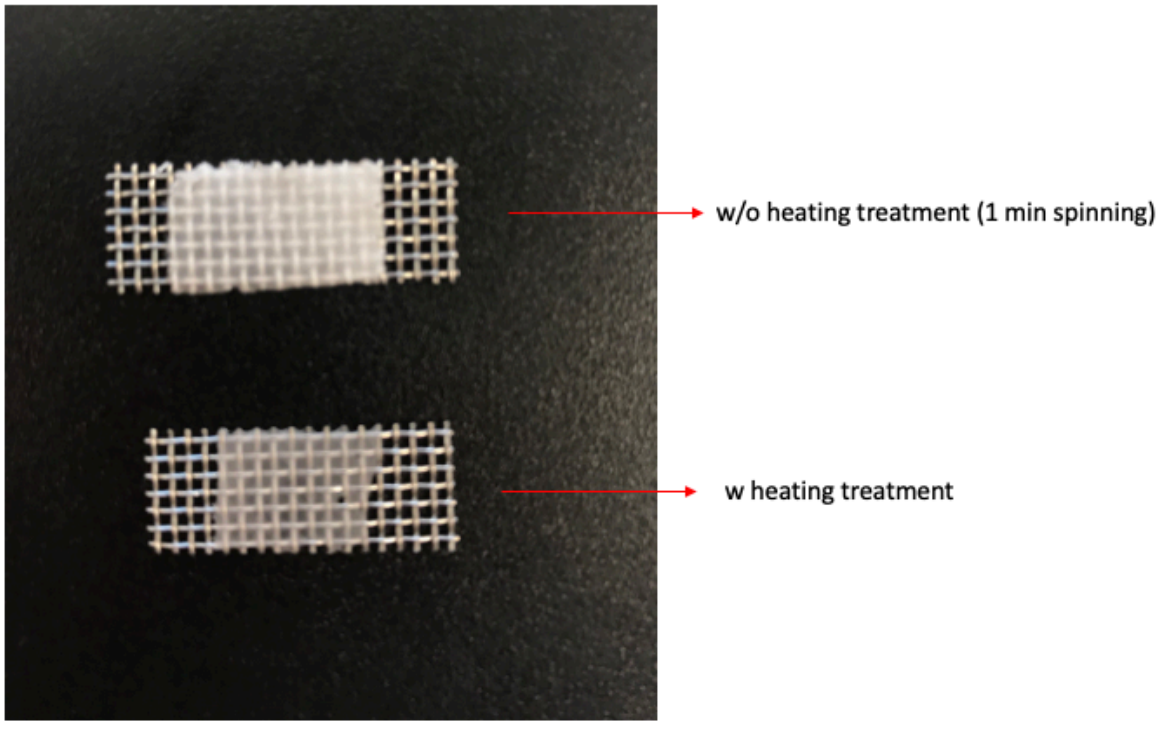

Figure 14. *Samples of cyanoacrylate electrospun membranes on stainless-steel mesh pre-and post-heating.*

The aim of the heat treatment was twofold. First, as a result of the much faster deposition, the degree of transparency was hardly controllable. An accurate heating process could partially melt

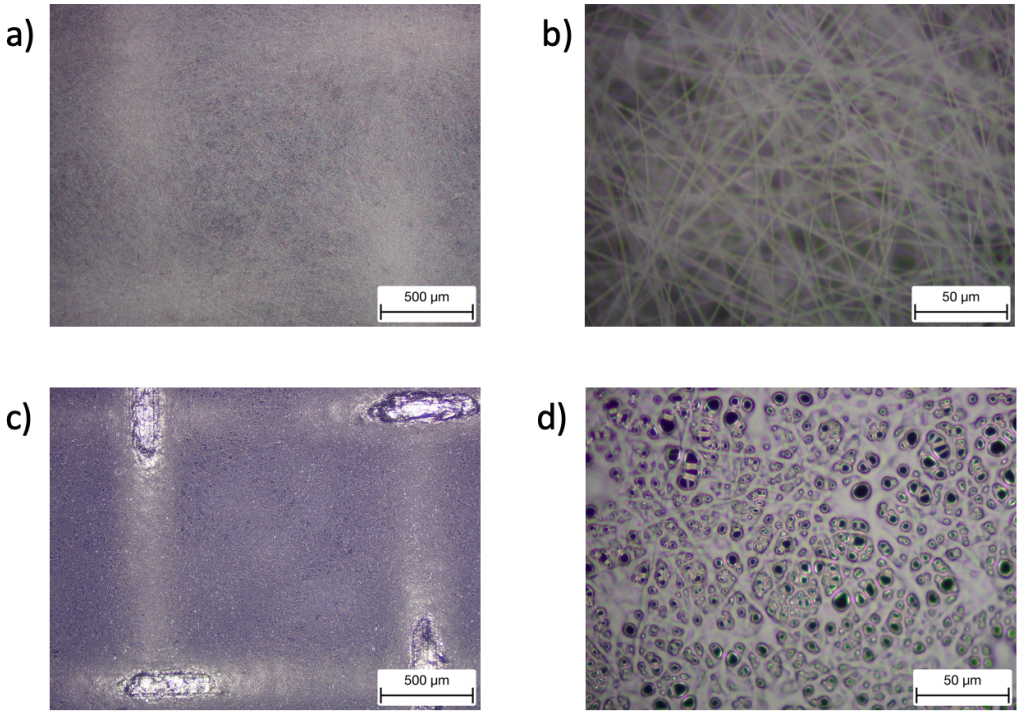

Figure 15. *Optical images of cyanoacrylate substrates (1 minute of spinning) before treatment* ***(a, b)*** *and after treatment* ***(c, d)****.*

fibers and help mitigating opacity. On the other hand, melted cyanoacrylate fibers occur in form of a semi-flat layer, with a much more defined porosity. Therefore, characterization of the substrates in terms of a mean porosity wasn't needed anymore, but a more precise porosity index could have been measured, with the process tuned accordingly.

The majority of cyanoacrylate samples showed a loss in structural integrity, within one week at most from the heating process, resulting in the appearance of cracks through the membrane (Figure 16). This phenomenon was possibly due to the treatment itself, and the consequent increased tensile strength between the melted fibers and the steel grid used as support. Therefore, cyanoacrylate was recognized as an unsuitable material for the project and was eventually discarded.

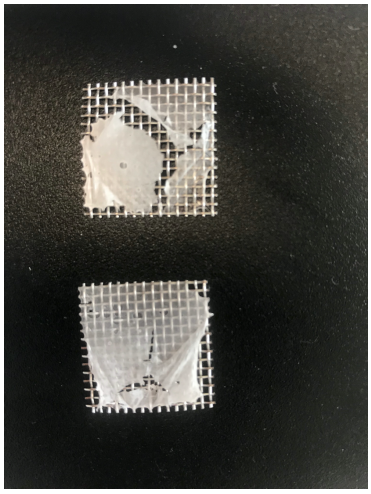

Figure 16. *Cracks forming on cyanoacrylate substrates following the heating treatment.*

3.2 *In vitro* BBB model characterization

Two-compartment BBB models consisting of electrospun fibrous CA scaffolds were used to culture brain endothelial cells (bEnd.3) at high confluence. The cells were cultivated on the top side of the fibrous membrane, which separates the luminal chamber (on the upper part) from the abluminal compartment (on the bottom).

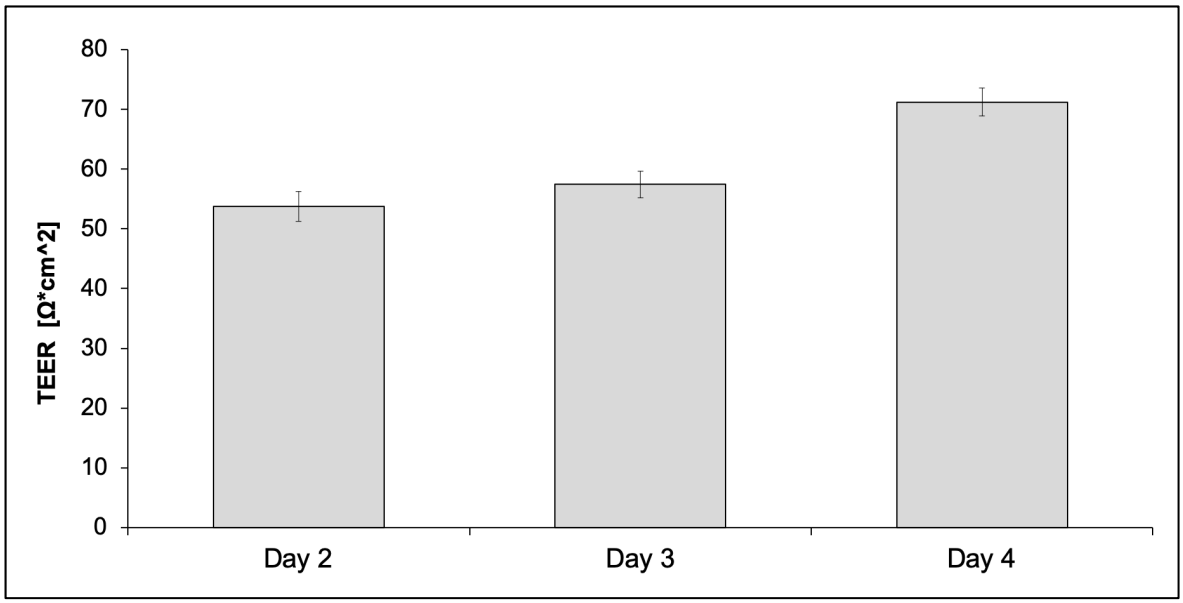

Figure 17. *Transendothelial electrical resistance (TEER) of in vitro blood-brain barrier (BBB) model developed on electrospun cellulose acetate (CA) scaffold.*

The BBB model transendothelial electrical resistance (TEER) was measured during each day of the culture (Figure 17). The values obtained were 53 ± 2 $\Omega \cdot cm^2$, 57 ± 2 $\Omega \cdot cm^2$ and 71 ± 2 $\Omega \cdot cm^2$, respectively on day 2, day 3 and day 4 of the culture. The constantly increasing value demonstrates both a good rate of cells proliferation and a proper trend in the barrier formation process.

The model permeability to FITC-dextran (4 kDa) was measured through a spectrofluorometer (Figure 18). The mean values for the cultures were 16806 ± 164371 counts at 10 min, 870117 ± 142673 counts at 30 min and 1057469 ± 306184 counts at 4 h. The mean values for the cell-free scaffolds were 2084064 ± 328741 counts at 10 min, 2426554 ± 285346 counts at 30 min and 3383901 ± 612369 counts at 4 h. The values for the cultures resulted to be significantly lower with

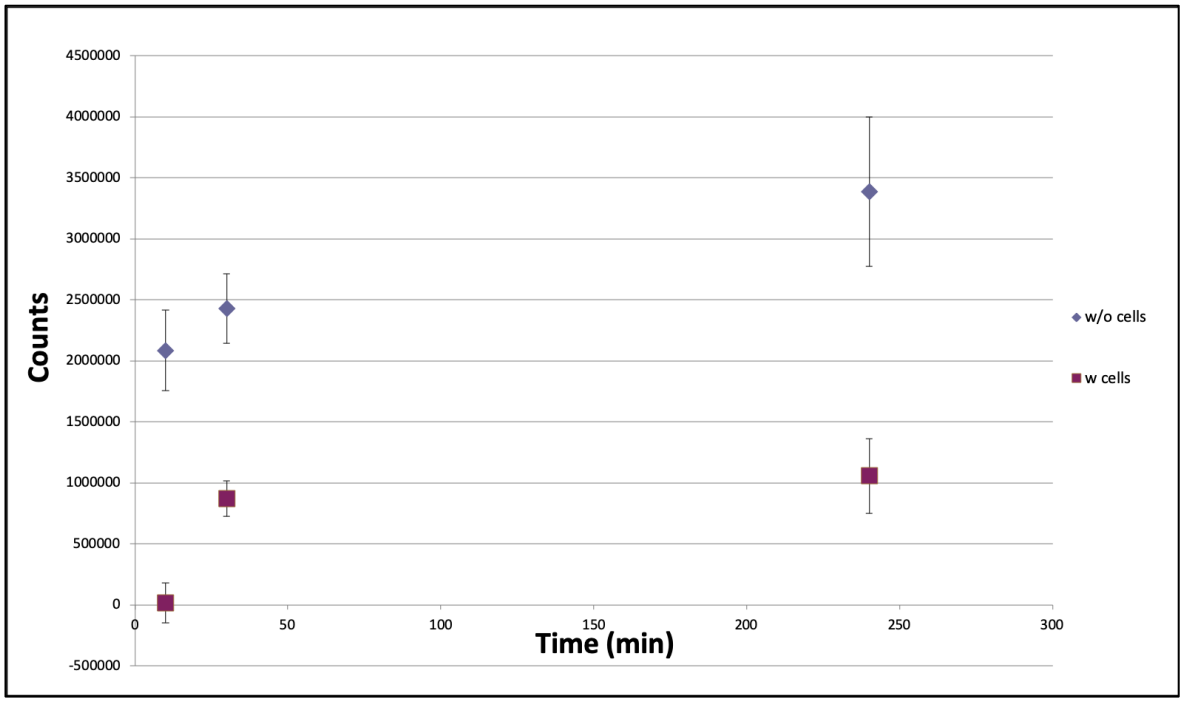

Figure 18. *Permeability of in vitro blood-brain barrier (BBB) to FITC-dextran.*

respect to the correspondent cell-free scaffold adopted as control, showing the developed barrier function of the model.

Confocal images of the models were obtained (Figure 19), showing both cells nuclei (Figure 19a) and cytoskeletal actin filaments (Figure 19b), and demonstrating the high confluence reached by proliferating cells. The image in Figure 20a (60X) was taken with the sample placed upside-down inside the microscope, thus showing a good degree of transparency of the model useful for possible further analysis. On the other hand, Figure 20b (20X) shows how the signal of cytoskeletal actin filaments (in green) partially overlaps with the one of CA fibers (in red), therefore indicating the cell-fiber interface. Therefore, such substrates constitute a good enough replica of the *in vivo* ECM. Lastly, the comparison of images in Figure 21 shows that, in addition to a high confluence of cells obtained on the surface of the membrane (Figure 21a), some cells were even found in the inside of the structure (Figure 21b), indicating that the model promotes cell migration.

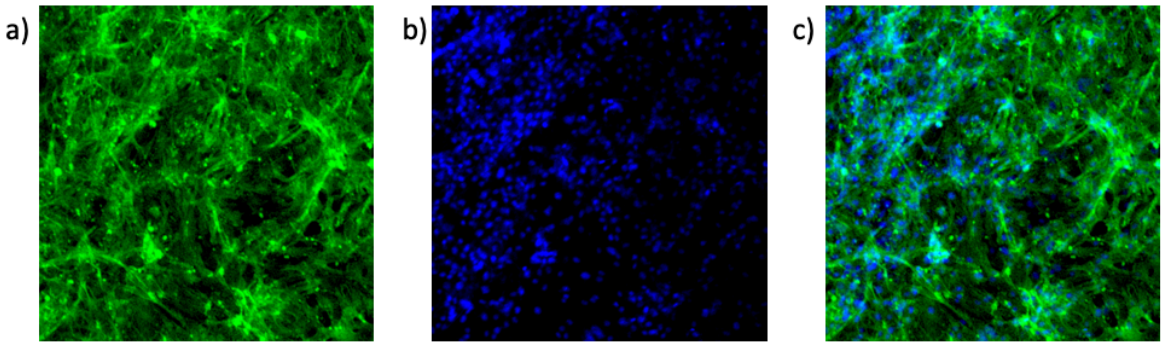

Figure 19. *Confocal images of the BBB model. Cytoskeletal actin filaments* **(a)**, *cells nuclei* **(b)** *and merge* **(c)**.

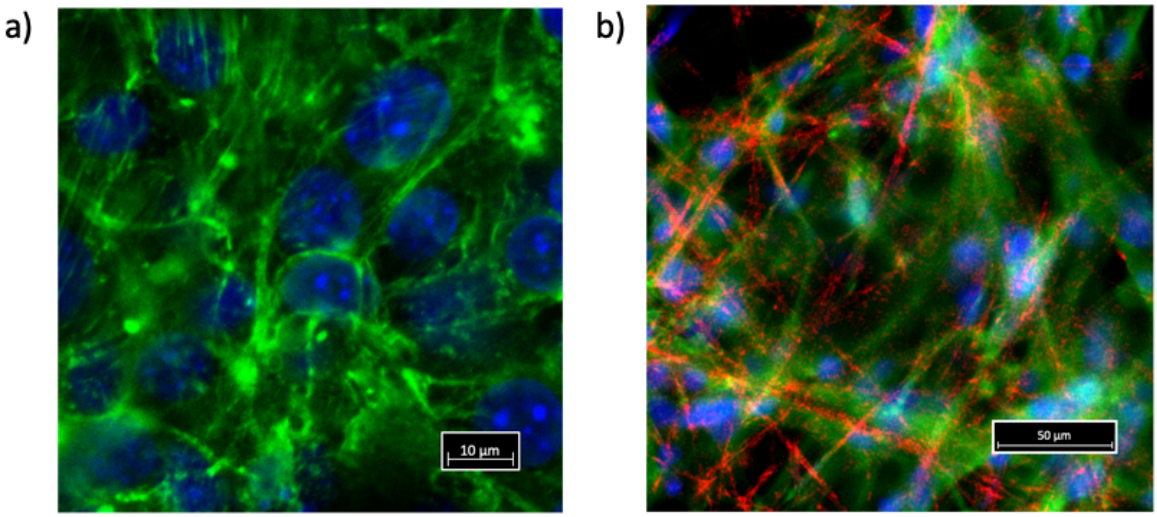

Figure 20. (a) *Confocal fluorescence imaging with an inverted microscope of the insert placed upside-down;* **(b)** *F-actin (green) and cellulose acetate (CA) fibers in red.*

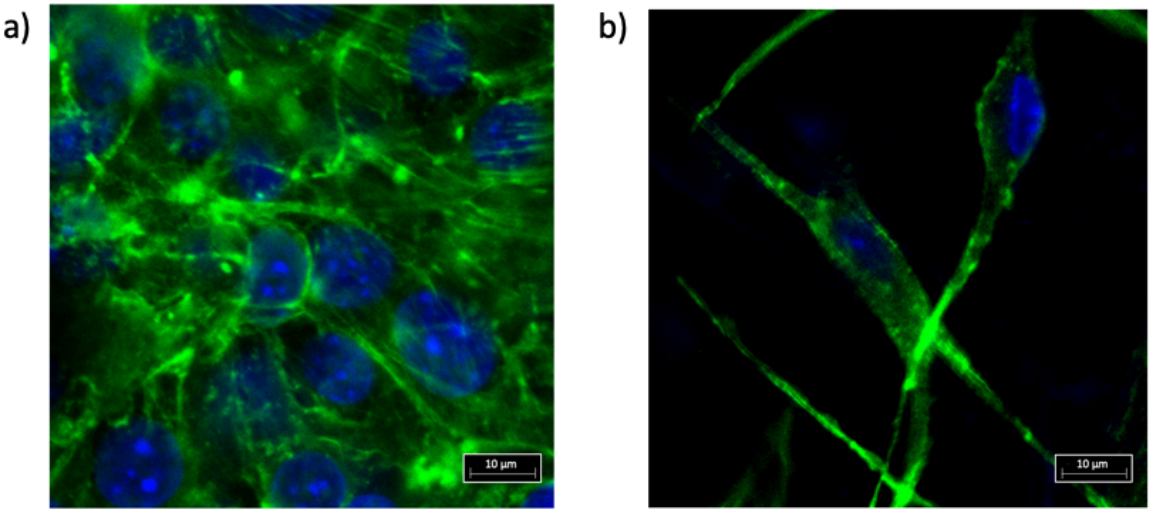

Figure 21. (a) *Endothelial cell layer developed on the fiber surface;* **(b)** *endothelial cells migrated inside the scaffold.*

4 Discussion

In this thesis, a new innovative approach for the development of a 2D static BBB *in vitro* model meant for high-throughput pharmaceutical screenings was evaluated. The approach exploits the technology of electrospinning that can be used to realize nano-fibrous biomimetic scaffolds.

The barrier functions showed by endothelial cells forming the walls of CNS blood vessel prevent most of the molecules meant to treat cerebral disorders to accumulate inside the brain parenchyma. Thus, proper treatment of CNS disorders and efficient drug delivery to the neural tissue across the BBB remain major challenges. The development of new methods for drug testing that are faster and less expensive is therefore a mandatory objective to promote the research of new solutions in the field of neural treatments.

The choice of electrospinning method to realize substrates for the model was due to a number of reasons. First of all, substrates prepared with this technique are made of polymeric nanometric fibers, arranged in a random way. Both fiber's dimension and arrangement mimic the structure of the native extracellular matrix (ECM) where cells normally reside and from which they receive the correct mechanical stimuli to differentiate, proliferate and fulfill their functions. Secondly, this method allows to a certain extent to control dimension and density of the deposited fibers by acting on process parameters such as spinning time and applied voltage. Therefore, substrate's features such as degree of transparency and mean porosity can be easily tuned. Lastly, the whole process is fast and economical, and the final product doesn't require any post-treatment.

The material chosen for the substrates was cellulose acetate. It is a naturally occurring polymer derived from cellulose, whose characteristics make it an optimal choice to be used in the electrospinning process. Moreover, due to its well-known biocompatibility, CA has a spectrum of utilities in the domain of biotechnologies widely recognized in literature. Different concentrations for the solution and different spinning times were tried, and the results were analyzed with optical and scanning electron microscopy in order to find the optimal combination. As can be seen, optical

images show a generally homogeneous distribution of fibers all throughout the metallic wire employed as support for the process, thus avoiding the formation of gradients of barrier properties that could later invalidate the results. SEM images, on the other hand, show no major defects to be present on the fibers (*e.g.* beads, ribbons…), demonstrating that both processing and solution parameters were tuned correctly. Substrates of the chosen kind were then used to replace the membrane of Transwell filters, to which they were fixed using PDMS, and then UV sterilized.

The BBB model was realized by seeding bEnd.3 cells at high confluence on the internal (luminal) side of the Transwell, that has previously been placed inside a well. Both luminal and abluminal side of the model were filled with high glucose medium, and the culture was carried out for 4 days in appropriate conditions.

The BBB model was investigated through the analysis of trans endothelial electrical resistance value and permeability to FITC-dextran. Measurements of TEER were taken on day 2, 3 and 4 of the culture. The increasing trend shows the consolidation of the barrier formation process, with a mean value of 71 ± 2 $\Omega \cdot cm^2$ on the last day, which is generally comparable to, if not better than, most of the cases of similar monolayer models found in literature. Permeability was assessed on the last day of the culture using 4 kDa FITC-dextran directly injected in the luminal compartment. Fluorescence emissions in the abluminal compartment were analyzed at different time points and the results show a significant difference between the BBB model and the cell-free control.

In this paragraph, the Electrospun CA model will be compared to other models of the blood-brain barrier commonly used for drug testing in literature. Starting with monoculture models, which represent the most direct benchmark for our model, it is necessary to analyse separately models based on primary cell cultures and models based on immortalized cell lines. Although the former employ primary cells derived from different mammals, focusing only on the usage of human primary cells the TEER values can be expected above 1000 $\Omega \cdot cm^2$ on confluent singular layers [87], which are higher than those obtained with the fibrous scaffold. However, the use of such models is restricted both by the lack of availability of experimental materials and time requirements, and the

tissue, acquired from autopsies or biopsies, often is not considered a healthy resource [88]. On the other hand, focusing on models made of immortalized cell lines, TEER values are more similar. Paradis *et al.* estimated the TEER value of hBMEC monolayers (human brain microvascular endothelial cells) to be between 20 and 200 $\Omega \cdot cm^2$ [89]. The same values are confirmed by Eigenmann *et al.* [90], showing mean TEER values for hBMEC monolayers to be between 20.7 and 33.3 $\Omega \cdot cm^2$. Both cultures were performed on commercial transparent PET membranes with 3-µm pore size. Co-culture models show higher TEER values (up to 500-600 $\Omega \cdot cm^2$) and lower permeability values compared with EC monocultures in general [91], and with our model in particular. Zhang *et al.* [92] developed an EC/astrocytes co-culture showing a TEER value of 340 $\Omega \cdot cm^2$, and Wilhelm *et al.* [93] a triple co-culture (EC, pericytes, astrocytes) showing mean TEER values of 264 ± 67 $\Omega \cdot cm^2$. For both cases, although higher values of TEER were reached, the model would probably benefit from the usage of our CA fibrous scaffold, since the substrates used in both cases were commercial Transwell© filters with a lower degree of biomimicry. The same is true for more complex dynamic models, like the humanized DIV-BBB developed by Cucullo and colleagues that employed human cerebral EC line (hCMEC/D3) grown in the lumen of microporous fibers (TEER of around 1000 $\Omega \cdot cm^2$) [94], or microfluidic models such as the chip studied by Griep *et al.* by using the same hCMEC/D3 cultured on a conventional Transwell© polycarbonate membrane separating two microfluidic compartments and exposed to fluid SS (TEER of around 36.9 ± 0.9 $\Omega \cdot cm^2$) [95]. However, in opposition to common static blood-brain barrier models, such apparatuses are not designed for high-throughput pharmaceutical studies [96].

Once the measurements were completed, cells were fixed in paraformaldehyde and stained for nuclei and cytoskeletal actin in order to be further analyzed through confocal imaging. Confocal images consequently taken show the high confluence reached by proliferating cells on the surface of the scaffold, with actin filaments and CA fibers oriented in the same direction. Cells found within the membrane show that cell migration was promoted as well. Both these two results demonstrate to a certain extent the similarity between the CA substrates and the native CNS ECM.

In summary, the proposed approach is a promising strategy to realize *in vitro* BBB models suitable for high-throughput analysis since the results are totally comparable with other widely employed monolayer models of the barrier, and cost and time requirements for the whole process are highly restricted.

5 Further Outlook and Conclusions

This thesis focuses on the design, preparation and characterization of an *in vitro* model of the BBB for drug development and testing. The process exploited the technology of electrospinning to fabricate substrates of cellulose acetate fibers. The BBB model was realized fixing the membranes at the opening of a Transwell filter. Cells of the bEnd.3 type were seeded at high confluence on the internal side and cultured in appropriate conditions for 4 days. Model's characterization was carried out by assessing TEER values during the culture and permeability to FITC-dextran on the last day. Finally, cells underwent fixation and staining in order for confocal imaging to be performed.

In continuation of this research, there is the intention to carry out a number of improvements for the model, as well as further analysis aimed at characterizing it better.

First of all, the model can be made more complex; a greater level of complexity can be achieved by adding one or more cellular components. As mentioned above, brain endothelial cells represent the principal component of BBB, but other types of cells have a crucial role in function and regulation of the barrier too. Consequently, a more complex model can be obtained if other cells (*i.e.* astrocytes/glial cells, pericytes and neurons) are employed. Glial-endothelial cell co-culture models are extensively used nowadays for studies on drug delivery as a result of glial cell's ability to induce BBB properties [92]. In vitro studies have demonstrated a strong relation between pericytes and the formation and maintenance of cerebral blood vessels system, and showed an increasing TEER as a result of the addition of this cell type [97]. Neurons, on the other hand, have been proved to promote the production of BBB enzymes in cultured cerebral ECs [98]. Generally, models that better mimic *in vivo* BBB anatomical features amongst co-culture models use ECs with astrocytes and/or pericytes [99] (Figure 22).

A second, and possibly complementary, approach could be the development of substrates with aligned CA fibers, employing a rotating and/or moving collector during the spinning step. The

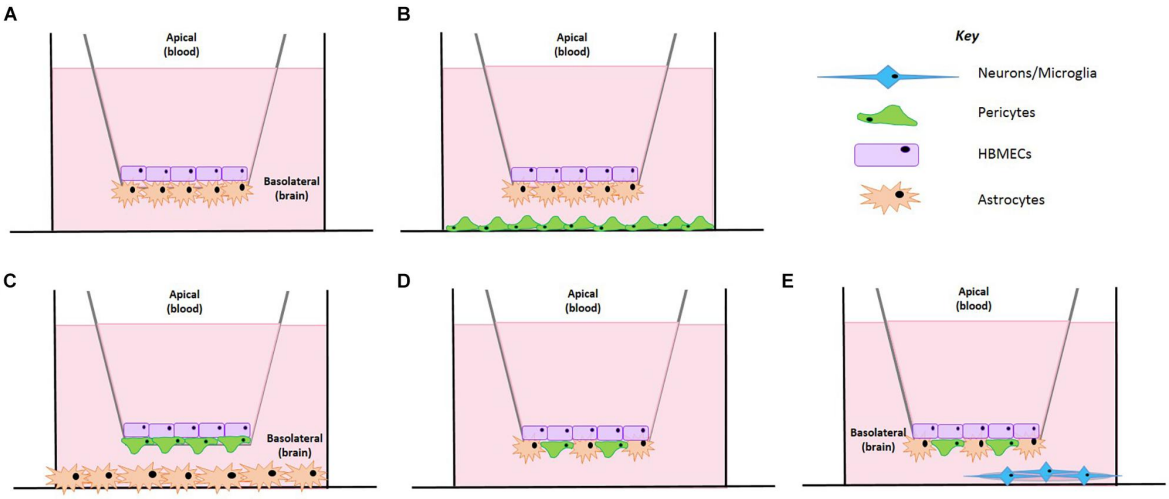

Figure 22. *Schematic representation of in vitro BBB models adopting different cell types.*

benefits of this approach could be two. First, the substrate's structure would be more controlled and reproducible, thus making the whole production process to be more scalable. Secondly, several studies have shown that cells cultured on aligned electrospun fibrous substrates exhibit contact guidance, partially highlighting the importance of an organized arrangement showed by collagen fibers that constitute many extracellular matrixes. Therefore, where ECM of a tissue is composed of oriented fibers (*e.g.* blood vessels), culturing their cells on aligned nanofibrous scaffolds may show responses that mimic that of the cells in their native environment [100].

Third, electrospun fibers could be further modified with the purpose of releasing growth factors or other drugs aimed to promote BBB development, such as vascular endothelial growth factor (VEGF) [101]. The easiest way to bind molecules to electrospun fibers is by physical adsorption (Figure 23a), in which electrostatic forces guide the biomolecules attachment to the scaffolds. However, this approach is rarely used due to the uncontrolled release profiles. On the other hand, covalent immobilization exploits chemical bonds formation to immobilizes biomolecules onto the fiber surface (Figure 23b). Compared to the former, the latter is predominantly used since the release of the immobilized molecules can be controlled by external enzymes [102].

Once the optimal version of the model will be found, studies can be carried out concerning the passage through the barrier of drug molecules and particles. Moreover, because of the cost- and

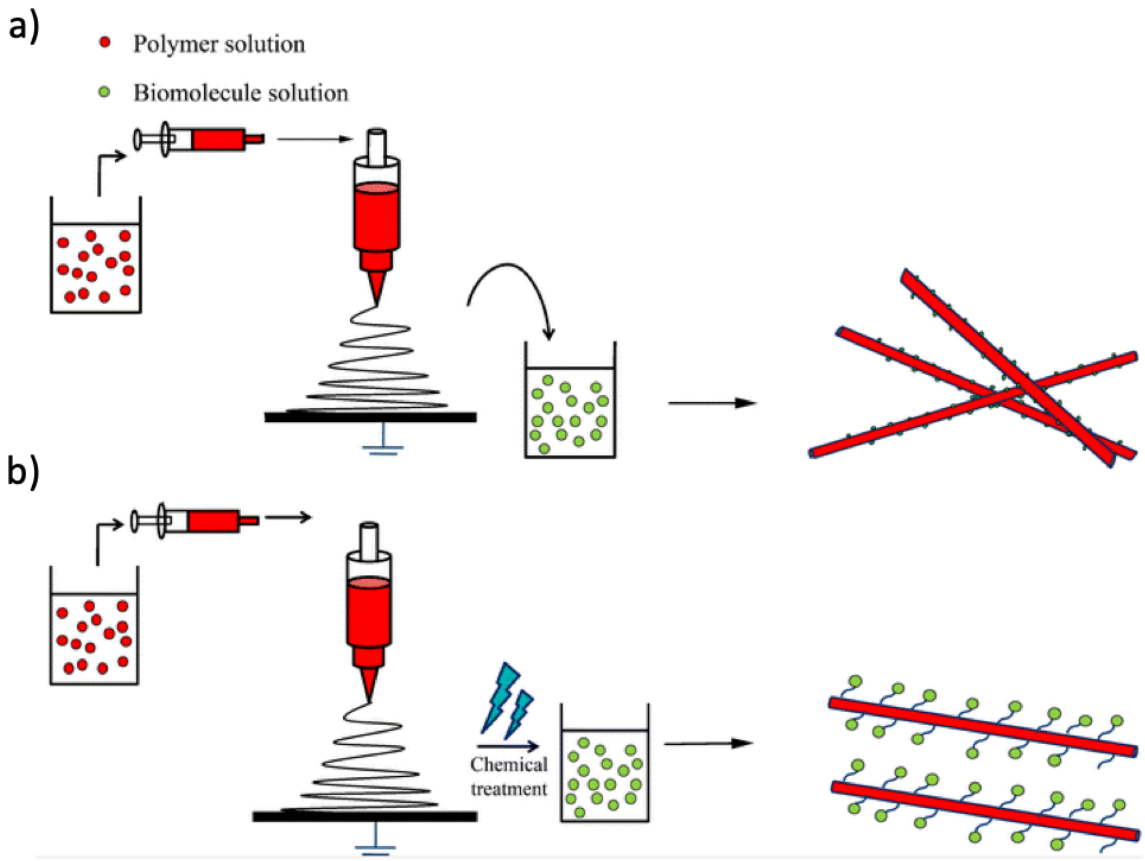

Figure 23. *Fabrication techniques of bioactive electrospun scaffolds.* **(a)** *physical adsorption;* **(b)** *covalent immobilization.*

time-effectiveness of the whole development process, the model could become suitable for drug discovery procedures that require large quantities of experimental test and an efficient cost control.

6 Bibliography

[1] N. J. Abbot, A. A. K. Patabendige, D. E. M. Dolman, S. R. Yusof and D. J. Begley, «Structure and function of the blood-brain barrier» *Neurobiology of Disease,* vol. 37, pp. 13-25, 2010.

[2] N. J. Abbott, L. Rönnbäck and E. Hansson, «Astrocyte–endothelial interactions at the blood–brain barrier» *Nature Rev. Neurosci.,* vol. 7, pp. 41-53, 2006.

[3] A. M. Palmer, «The blood-brain barrier» *Neurobiology of Disease,* vol. 37, pp. 1-2, 2010.

[4] B. V. Zlokovic, «The blood-brain barrier in health and cronic neurodegenerative disorders» *Neuron,* vol. 57, pp. 178-201.

[5] R. Daneman and A. Prat, «The blood-brain barrier» *Cold Spring Harb Perspect Biol,* vol. 7, pp. 2-5, 2015.

[6] D. E. Sims, «The pericyte—A review» *Tissue Cell,* vol. 18, pp. 153-174, 1986.

[7] A. Armulik, G. Genové, M. Mae, M. H. Nisancioglu, E. Wallgard, C. Niaudet, L. He, J. Norlin, P. Lindblom and K. Strittmatter, «Pericytes regulate the blood–brain barrier» *Nature,* vol. 468, pp. 557-561, 2010.

[8] G. J. Del Zoppo, R. Milner, T. Mabuchi, S. Hung, X. Wang and J. A. Koziol, «Vascular matrix adhesion and the blood–brain barrier» *Biochem Soc Trans,* vol. 34, pp. 1261-1266, 2006.

[9] R. C. Janzer and M. C. Raff, «Astrocytes induce blood – brain barrier properties in endothelial cells» *Nature,* vol. 325, pp. 253-257, 1987.

[10] H. Wolburg and A. Lippoldt, «Tight junctions of the blood–brain barrier: development, composition and regulation» *Vascul. Pharmacol.,* vol. 38, pp. 323-337, 2002.

[11] C. M. Van Itallie and J. M. Anderson, «Claudins and epithelial paracellular transport» *Annu Rev Physiol ,* vol. 68, pp. 403-429, 2006.

[12] A. M. Butt, H. C. Jones and N. J. Abbott, «Electrical resistance across the blood–brain barrier in anaesthetised rats: a developmental study» *J. Physiol. ,* vol. 429, pp. 47-62, 1990.

[13] W. M. Pardridge, «Drug transport across the blood–brain barrier» *J. Cereb. Blood Flow Metab.,* vol. 32, n. 11, pp. 1959-1972, 2012.

[14] M. De Bock, V. Van Haver, R. E. Vandenbroucke, E. Decrock, N. Wang eand L. Leybaert, «Into Rather Unexplored Terrain—Transcellular Transport Across the Blood–Brain Barrier» *Glia,* vol. 64, pp. 1097-1123, 2016.

[15] A. Hayer, M. Stoeber, D. Ritz, S. Engel, H. H. Meyer and A. Helenius, «Caveolin-1 is ubiquitinated and targeted to intralumenal vesicles in endolysosomes for degradation» *J Cell Biol,* vol. 191, p. 615–629, 2010.

[16] N. Strazielle and J. F. Ghersi-Egea, «Physiology of blood–brain interfaces in relation to brain disposition of small compounds and macromolecules» *Mol Pharm,* vol. 10, p. 1473–1491, 2013.

[17] J. L. Mikitsh and A. M. Chacko, «Pathways for small molecule delivery to the central nervous system across the blood–brain barrier» *Perspect Medicin Chem,* vol. 6, pp. 11-24, 2014.

[18] N. J. Abbott, «Blood–brain barrier structure and function and the challenges for CNS drug delivery» *J. Inherit. Metab. Dis.,* vol. 36, n. 3, p. 437–449, 2013.

[19] S. M. Stamatovic, N. Sladojevic, R. F. Keep and A. Andjelkovic, «Blood–brain barrier permeability: From bench to bedside» 2011.

[20] K. Park, «Trojan monocytes for improved drug delivery to the brain» *J. Control. Release,* vol. 132, n. 2, p. 75, 2008.

[21] C. Crone, «Facilitated transfer of glucose from blood into brain tissue» *J Physiol,* vol. 181, pp. 103-113, 1965.

[22] W. M. Pardridge and R. J. Boado, «Reengineering biopharmaceuticals for targeted delivery across the blood-brain barrier» *Methods Enzymol,* vol. 503, p. 269–292, 2012.

[23] S. Wohlfart, S. Gelperina and J. Kreuter, «Transport of drugs across the blood–brain barrier by nanoparticles» *Journal of Controlled Release ,* vol. 161, pp. 264-273, 2012.

[24] j. Banerjee, Y. Shi and H. S. Azevedo, «In vitro blood–brain barrier models for drug research: state-of-the-art and new perspectives on reconstituting these models on artificial basement membrane platforms» *Drug Discovery Today ,* vol. 21, n. 9, pp. 1367-1386, 2016.

[25] S. Aday, R. Cecchelli, D. Hallier-Vanuxeem, M. P. Dehouck and L. Ferreira, «Stem Cell-Based Human Blood–Brain Barrier Models for Drug Discovery and Delivery» *Trends Biotechnol. ,* vol. 34, pp. 382-393, 2016.

[26] H. C. Helms, N. J. Abbott, M. Burek, R. Cecchelli, P. Couraud, M. A. Deli, C. Forster, H. J. Galla, I. A. Romero, E. V. Shusta, M. J. Stebbins, E. Vandenhaute, B. Weksler and B. Brodin, «In vitro models of the blood–brain barrier: An overview of commonly used brain endothelial cell culture models and guidelines for their use» *Journal of Cerebral Blood Flow & Metabolism,* vol. 36, n. 5, p. 862–890, 2016.

[27] F. Joo and I. Karnushina, «A procedure for the isolation of capillaries from rat brain» *Cytobios,* vol. 8, pp. 41-48, 1973.

[28] M. Deli, «Blood-brain barrier models» *Handbook of Neurochemistry and Molecular Neurobiology: Neural Membranes and Transport ,* pp. 29-55, 2007.

[29] R. C. Janzer and M. C. Raff, «Astrocytes induce blood–brain barrier properties in endothelial cells» *Nature,* vol. 325, pp. 253-257.

[30] A. Wolff, M. Antfolk, B. Brodin and M. Tenje, «In Vitro Blood–Brain Barrier Models—An Overview of Established Models and New Microfluidic Approaches» *Journal of Pharmaceutical Sciences,* vol. 104, n. 9, pp. 2727-2746, 2015.

[31] R. Daneman, L. Zhou, A. A. Kebede and B. A. Barres, «Pericytes are required for blood–brain barrier integrity during embryogenesis» *Nature,* vol. 468, pp. 562-566, 2010.

[32] Q. Xue, Y. Liu, H. Qi, Q. X. L. Ma, W. Chen, G. Chen and X. Xu, «A Novel Brain Neurovascular Unit Model with Neurons, Astrocytes and Microvascular Endothelial Cells of Rat» *Int. J. Biol. Sci.,* vol. 9, p. 174, 2013.

[33] B. B. Weksler, E. A. Subileau, N. Perrière, P. Charneau, K. Holloway, M. Leveque, H. Tricoire-Leignel, A. Nicotra, S. Bourdoulous, P. Turowski, D. K. Male, F. Roux, J. Greenwood, I. A. Romero and P. O. Couraud, «Blood-brain barrier-specific

properties of a human adult brain endothelial cell line» *FASEB J,* vol. 19, n. 12, pp. 1872-1874, 2005.

[34] D. E. Eigenmann, G. Xue, K. S. Kim, A. V. Moses, M. Hamburger and M. Oufir, «Comparative study of four immortalized human brain capillary endothelial cell lines, hCMEC/D3, hBMEC, TY10, and BB19, and optimization of culture conditions, for an in vitro blood–brain barrier model for drug permeability studies» *Fluids and Barriers of the CNS,* vol. 10, pp. 1-17, 2013.

[35] E. S. Lippmann, A. Al-Ahmad, S. M. Azarin, S. P. Palecek and E. V. Shusta, «A retinoic acid-enhanced, multicellular human blood-brain barrier model derived from stem cell sources» *Sci. Rep.,* vol. 4, p. 4160, 2014.

[36] E. S. Lippman, S. M. Azarin, J. E. Kay, R. A. Nessler, H. K. Wilson, A. Al-Ahmad, S. P. Palecek and E. V. Shusta, «Derivation of blood-brain barrier endothelial cells from human pluripotent stem cells» *Nature Biotechnology,* vol. 30, p. pages 783–791, 2012.

[37] P. Naik and L. Cucullo, «In Vitro Blood–Brain Barrier Models: Current and Perspective Technologies Author links open overlay panel» *Journal of Pharmaceutical Sciences,* vol. 101, pp. 1337-1354, 2012.

[38] A. Marino, O. Tricinci, M. Battaglini, C. Filippeschi, V. Mattoli, E. Sinibaldi and G. Ciofani, «A 3D Real-Scale, Biomimetic, and Biohybrid Model of the Blood-Brain Barrier Fabricated through Two-Photon Lithography» *Small,* vol. 14, n. 6, 2018.

[39] J. Mensch, J. Oyarzabal, C. Mackie and P. Augustijns, «In vivo, in vitro and in silico methods for small molecule transfer across the BBB» *J. Pharm. Sci.,* vol. 98, pp. 4429-4468, 2009.

[40] J. Bicker, G. Alves, A. Fortuna and A. Falcao, «Blood–brain barrier models and their relevance for a successful development of CNS drug delivery systems: A review» *European Journal of Pharmaceutics and Biopharmaceutics ,* vol. 87, pp. 409-432, 2014.

[41] X. Liu, C. Chen and B. J. Smith, «Progress in brain penetration evaluation in drug discovery and development» *J. Pharmaco. Exp. Ther.,* vol. 325, pp. 349-356, 2008.

[42] J. A. Nicolazzo, S. A. Charman and W. N. Charman, «Methods to assess drug permeability across the blood–brain barrier» *J. Pharm. Pharmacol.,* vol. 58, pp. 281-293, 2006.

[43] L. Di, E. H. Kerns and G. T. Carter, «Strategies to assess blood–brain barrier penetration» *Expert Opin. Drug Discov.,* vol. 3, pp. 677-687, 2008.

[44] W. Loscher and H. Potschka, «Role of drug efflux transporters in the brain for drug disposition and treatment of brain diseases» *Prog. Neurobiol.,* vol. 76, pp. 22-76, 2005.

[45] D. B. Stanimirovic, M. Bani-Yaghoub, M. Perkins and A. S. Haqqani, «Blood-brain barrier models: in vitro to in vivo translation in preclinical development of CNS-targeting biotherapeutics» *Expert Opin. Drug Discov.,* vol. 10, 2014.

[46] M. K. DeSalvo, N. Mayer, F. Mayer and R. J. Bainton, «Physiologic and anatomic characterization of the brain surface glia barrier of Drosophila» *Glia,* vol. 59, pp. 1322-1340, 2011.

[47] M. A. Pickart and E. W. Klee, «Zebrafish approaches enhance the translational research tackle box» *Transl Res,* vol. 163, pp. 65-78, 2014.

[48] K. Watanabe, Y. Nishimura, T. Nomoto, N. Umemoto, Z. Zhang, B. Zhang, J. Kuroyanagi, Y. Shimada, T. Shintou, M. Okano, T. Miyazaki, T. Imamura and T. Tanaka, «In vivo assessment of the permeability of the blood-brain barrier and blood-retinal barrier to fluorescent indoline derivatives in zebrafish» *BMC Neurosci.,* vol. 13, n. 101, 2012.

[49] A. M. Stewart, O. Braubach, J. Spitsbergen, R. Gerlai and A. V. Kalueff, «Zebrafish models for translational neuroscience research: from tank to bedside» *Trends Neurosci.,* vol. 37, n. 5, pp. 264-278, 2014.

[50] Y. Chen and L. Liu, «Modern methods for delivery of drugs across the blood–brain barrier» *Adv. Drug Deliv. Rev.,* vol. 64, pp. 640-665, 2012.

[51] M. M. Patel, B. R. Goyal, S. V. Bhadada, J. S. Bhatt and A. F. Amin, «Getting into the brain: approaches to enhance brain drug delivery» *CNS Drugs,* vol. 23, pp. 35-58, 2009.

[52] J. Correale and A. Villa, «Cellular elements of the blood–brain barrier» *Neurochem. Res.,* vol. 34, pp. 2067-2077, 2009.

[53] S. Krol, «Challenges in drug delivery to the brain: nature is against us» *J. Control. Release,* vol. 164, pp. 145-155, 2012.

[54] R. Rempe, S. Cramer, S. Huwel and H. J. Galla, «Transport of Poly(n-butylcyano-acrylate) nanoparticles across the blood–brain barrier in vitro and their influence on barrier integrity» *Biochem. Biophys. Res. Commun.,* vol. 406, pp. 64-69, 2011.

[55] A. Formhals, «Process and apparatus for preparing artificial threads». United States Brevetto 1,975,504, 1934.

[56] G. Taylor, «Electrically driven jets» *Proc Natl Acad Sci ,* vol. a313, n. 1515, pp. 453-475, 1969.

[57] A. Rogina, «Electrospinning process: Versatile preparation method for biodegradable and natural polymers and biocomposite systems applied in tissue engineering and drug delivery» *Applied Surface Science,* vol. 296, pp. 221-230, 2014.

[58] T. J. Sill and H. A. von Recum, «Electrospinning: Applications in drug delivery and tissue engineering» *Biomaterials,* vol. 29, pp. 1986-2006, 2008.

[59] J. Zhu, Y. Zhang, H. Shao and X. Hu, «Electrospinning and rheology of regenerated Bombyx mori silk fibrion aqueous solutions: The effect of pH and concentration» *Polymer,* vol. 49, pp. 2880-2885, 2008.

[60] S. Megelski, J. S. Stephens, D. B. Chase and J. F. Rabolt, «Micro-andnanostructured surface morphology on electrospun polymer fibers» *Macromolecules,* vol. 35, n. 22, pp. 8456-8466, 2002.

[61] P. Baumgarten, «Electrostatic spinning of acrylic microfibers» *J Colloid Interface Sci,* vol. 36, n. 1, pp. 71-79, 1971.

[62] J. M. Deitzel, J. Kleinmeyer, D. Harris and N. C. B. Tan, «The effect of processing variables on the morphology of electrospun nanofibers and textiles» *Polymer,* vol. 42, n. 1, pp. 261-272, 2001.

[63] J. Zhou, C. Cao and X. Ma, «Anoveltree-dimensionaltubularscaffoldpreparedfrom silk fibroin by electrospinning» *Int. J. Biol. Macromol.,* vol. 45, pp. 504-510, 2009.

[64] J. Doshi and D. H. Reneker, «Electrospinning process and applications of electrospun fibers» *J Electrostatics,* vol. 35, n. 2-3, pp. 151-160, 1995.

[65] A. Greiner and J. H. Wendorff, «Electrospinning: A fascinating method for the preparation of ultrathin fibers» *Angew. Chem.,* vol. 46, pp. 5670-5703, 2007.

[66] T. G. Kim and T. G. Park, «Biomimicking extracellular matrix: cell adhesive RGD peptide modified electrospun poly(D,L-lactic-co-glycolic acid) nanofiber mesh» *Tissue Eng,* vol. 12, n. 2, pp. 221-233, 2006.

[67] H. Inoguchi, I. K. Kwon, E. Inoue, K. Takamizawa, Y. Maehara and T. Matsuda, «Mechanical responses of a compliant electrospun poly(L-lactide-co- epsilon-caprolactone) small-diameter vascular graft» *Biomaterials,* vol. 27, n. 8, pp. 1470-1478, 2006.

[68] H. Nie and C. H. Wang, «Fabrication and characterization of PLGA/HAp composite scaffolds for delivery of BMP-2 plasmid DNA» *J Control Release,* vol. 120, n. 1-2, pp. 111-121, 2007.

[69] F. Yang, R. Murugan, S. Wang and S. Ramakrishna, «Electrospinning of nano/ microscale poly(L-lactic acid) aligned fibers and their potential in neural tissue engineering» *Biomaterials,* vol. 26, n. 15, pp. 2603-2610, 2005.

[70] H. W. Ouyang, J. C. Goh, A. Thambyah, S. H. Teoh and E. H. Lee, «Knitted poly-lactide-co-glycolide scaffold loaded with bone marrow stromal cells in repair and regeneration of rabbit Achilles tendon» *Tissue Eng,* vol. 9, n. 3, pp. 431-439, 2003.

[71] T. T. T. Nguyen, C. Ghosh, S. -G. Hwang, N. Chanunpanich and J. S. Park, «Porous core/sheath composite nanofibers fabricated by coaxial electrospinning as a potential mat for drug release system» *Int. J. Pharm.,* vol. 439, pp. 296-306, 2012.

[72] The Editors of Encyclopaedia Britannica, «ENCYCLOPÆDIA BRITANNICA» 20 July 1998. [Online]. Available: https://www.britannica.com/science/cellulose-acetate. [Consultato il giorno May 2019].

[73] Q. P. Pham, U. Sharma and A. G. Mikos, «Electrospinning of polymeric nanofibers for tissue engineering applications: a review» *Tissue Eng,* vol. 12, n. 5, pp. 1197-1211, 2006.

[74] R. Konwarh, N. Karak and M. Misra, «Electrospun cellulose acetate nanofibers: The present status and gamut of biotechnological applications» *Biotechnology Advances,* vol. 31, pp. 421-437, 2013.

[75] P. Taepaiboon, U. Rungsardthong and P. Supaphol, «Vitamin-loaded electrospun cellulose ac- etate nanofiber mats as transdermal and dermal therapeutic agents for vitamin A acid and vitamin E» *Eur J Pharm Biopharm,* vol. 67, p. 387, 2007.

[76] X. J. Huang, P. C. Chen, F. Huang, Y. Ou, M. R. Chen and Z. K. Xu, «Immobilization of Candida rugosa lipase on electrospun cellulose nanofiber membrane» *J Mol Catal B: Enzym,* Vol. %1 di %23-4, pp. 95-100, 2011.

[77] C. Hellmann, A. Greiner and J. H. Wendorff, «Design of pheromone releasing nanofibers for plant protection» *Polym Adv Technol,* vol. 22, n. 4, pp. 407-413, 2011.

[78] K. Rodríguez, S. Renneckar and P. Gatenholm, «Biomimetic calcium phosphate crystal mineraliza- tion on electrospun cellulose-based scaffolds» *ACS Appl Mater Interfaces,* vol. 3, pp. 681-689, 2011.

[79] D. A. Rubenstein, S. M. Venkitachalam, D. Z. FangWang, H. Lu, M. D. Frame and W. Yin, «In vitro bio- compatibility of sheath–core cellulose-acetate-based electrospun scaffolds towards endothelial cells and platelets» *J Biomater Sci Polym Ed,* vol. 21, n. 13, pp. 1713-1736, 2010.

[80] S. J. Eichhorn, J. E. Gough and J. Dugan, «Aligned cellulose nanostructures for controlled tissue growth» in *Abstracts of Papers, 239th ACS National Meeting*, United States: San Francisco, CA, 2010.

[81] R. M. Faulks and S. Southon, «Assessing the bioavailability of nutraceuticals» in *Delivery and controlled release of bioactives in foods and nutraceuticals*, New York: CRC Press, 2008.

[82] S. Wongsasulak, M. Patapeejumruswong, J. Weiss, P. Supaphol and T. Yoovidhya, «Electrospinning of food-grade nanofibers from cellulose acetate and egg albumen blends» *J Food Eng,* vol. 98, pp. 370-376, 2010.

[83] X. Wang, Y.-G. Kim, C. Drew, B.-C. Ku, J. Kumar and L. A. Samuelson, «Electrostatic assembly of conjugated polymer thin layers on electrospun nanofibrous membranes for bio- sensors» *Nano Lett,* vol. 4, pp. 331-334, 2004.

[84] W. K. Son, J. H. Youk and W. H. Park, «Antimicrobial cellulose acetate nanofibers containing silver nanoparticles» *Carbohydr Polym,* vol. 65, pp. 430-434, 2006.

[85] Y. Tian, M. Wu, R. Liu, Y. Li, D. Wang, J. Tan, R. Wue and Y. Huang, «Electrospun membrane of cellulose acetate for heavy metal ion adsorption in water treatment» *Carbohyd Polym,* vol. 83, pp. 743-748, 2011.

[86] S. Xiao, S. Wu, M. Shen, R. Guo, Q. Huang, S. Wang and X. Shi, «Polyelectrolyte multilayer-assisted immobilization of zero-valent iron nanoparticles onto polymer nanofibers for potential environmental applications» *ACS Appl Mater Interfaces,* vol. 1, n. 12, pp. 2848-2855, 2009.

[87] M. J. Bernas, F. L. Cardoso, S. K. Daley, M. E. Weinand, A. R. Campos, A. J. G. Ferreira, J. B. Hoying, M. H. Witte, D. Brites, Y. Persidsky, S. H. Ramirez and M. A. Brito, «Establishment of primary cultures of human brain microvascular endothelial cells to provide an in vitro cellular model of the blood-brain barrier» *Nature Protocols,* n. 5, pp. 1265-1272, 2010.

[88] I. Wilhelm and I. A. Krizbai, «In vitro models of the blood-brain barrier for the study of drug delivery to the brain» *Molecular Pharmaceutics,* vol. 11, n. 7, pp. 1949-1963, 2014.

[89] A. Paradis, D. Leblanc and N. Dumais, «Optimization of an in vitro human blood–brain barrier model: Application to blood monocyte transmigration assays» *MethodsX,* vol. 3, pp. 25-34, 2016.

[90] D. E. Eigenmann, E. A. Jähne, M. Smieško, M. Hamburger and M. Oufir, «Validation of an immortalized human (hBMEC) in vitro blood-brain barrier model» *Anal Bioanal Chem,* vol. 408, p. 2095, 2016.

[91] G. Zysk, B. K. Schneider-Wald, J. H. Hwang, L. Bejo, K. S. Kim, T. J. Mitchell, R. Hakenbeck and H. P. Heinz, «Pneumolysin is the main inducer of cytotoxicity to brain microvascular endothelial cells caused by Streptococcus pneumoniae» *Infection and Immunity,* vol. 69, n. 2, pp. 845-852, 2001.

[92] Z. Zhang, A. J. McGoron, E. T. Crumpler and C. Z. Li, «Co-culture based blood-brain barrier in vitro model, a tissue engineering approach using immortalized cell lines

for drug transport study» *Applied Biochemistry and Biotechnology,* vol. 163, n. 2, pp. 278-295, 2011.

[93] I. Wilhelm, C. Fazakas and I. A. Krizbai, «In vitro models of the bloodebrain barrier» *Acta Neurobiologiae Experimentalis,* vol. 71, pp. 113-128, 2011.

[94] L. Cucullo, P. O. Couraud, B. Weksler, I. A. Romero, M. Hossain and E. Rapp, «Immortalized human brain endothelial cells and flow-based vascular modeling: a marriage of convenience for rational neurovascular studies» *Journal of Cerebral Blood Flow Metabolism,* vol. 28, n. 2, pp. 312-328, 2008.

[95] L. M. Griep, F. Wolbers, B. de Wagenaar, P. M. ter Braak, B. B. Weksler and I. A. Romero, «BBB on chip: microfluidic platform to mechanically and biochemically modulate bloodebrain barrier function» *Biomedical Microdevices,* vol. 15, n. 1, pp. 145-150, 2013.

[96] P. Naik and L. Cucullo, «In vitro bloodebrain barrier models: current and perspective technologies» *Journal of Pharmaceutical Science ,* vol. 101, n. 4, pp. 1337-1354, 2012.

[97] S. Santaguida, D. Janigro, M. Hossain, E. Oby, E. Rapp and L. Cucullo, «Side by side comparison between dynamic versus static models of bloodebrain barrier in vitro: a permability study» *Brain Research,* vol. 1109, n. 1, pp. 1-13, 2006.

[98] U. Tontsch and H. C. Bauer, «Glial cells and neurons induce bloodebrain barrier related enzymes in cultured cerebral endothelial cell» *Brain Research,* vol. 539, pp. 247-253, 1991.

[99] B. Sarmento, «Cell-based in vitro models for studying bloodebrain barrier (BBB) permeability» in *Concepts and Models for Drug Permeability Studies - Cell and Tissue Based in vitro Culture Models*, 2015, pp. 169-188.

[100] W. Teo, «Influence of fiber alignment on cells and tissue regeneration» 10 November 2015. [Online]. Available: http://electrospintech.com/cellalignfibers.html#.XW0zO1BS8nd. [Consultato il giorno 1 September 2019].

[101] S. Nag, J. L. Takahashi and D. W. Kilty, «Role of vascular endothelial growth factor in blood-brain barrier breakdown and angiogenesis in brain trauma» *J Neuropathol Exp Neurol.,* vol. 56, n. 8, pp. 912-921, 1997.

[102] W. Ji, Y. Sun, F. Yang, J. J. J. van den Beucken, M. Fan, Z. Chen and J. A. Jansen, «Bioactive Electrospun Scaffolds Delivering Growth Factors and Genes for Tissue Engineering Applications» *Pharmaceutical Research,* vol. 28, n. 6, pp. 1259-1272, 2011.

[103] L. M. Griep, F. Wolbers, B. de Wagenaar, P. M. ter Braak, B. B. Weksler, I. A. Romero, P. O. Couraud, I. Vermes, A. D. van der Meer and A. van der Berg, «BBB ON CHIP: microfluidic platform to mechanically and biochemically modulate blood-brain barrier function» *Biomedical Microdevices,* vol. 15, pp. 145-150, 2013.